Bifurcation Analysis of a Marine Food Chain

Flora Souza Bacelar

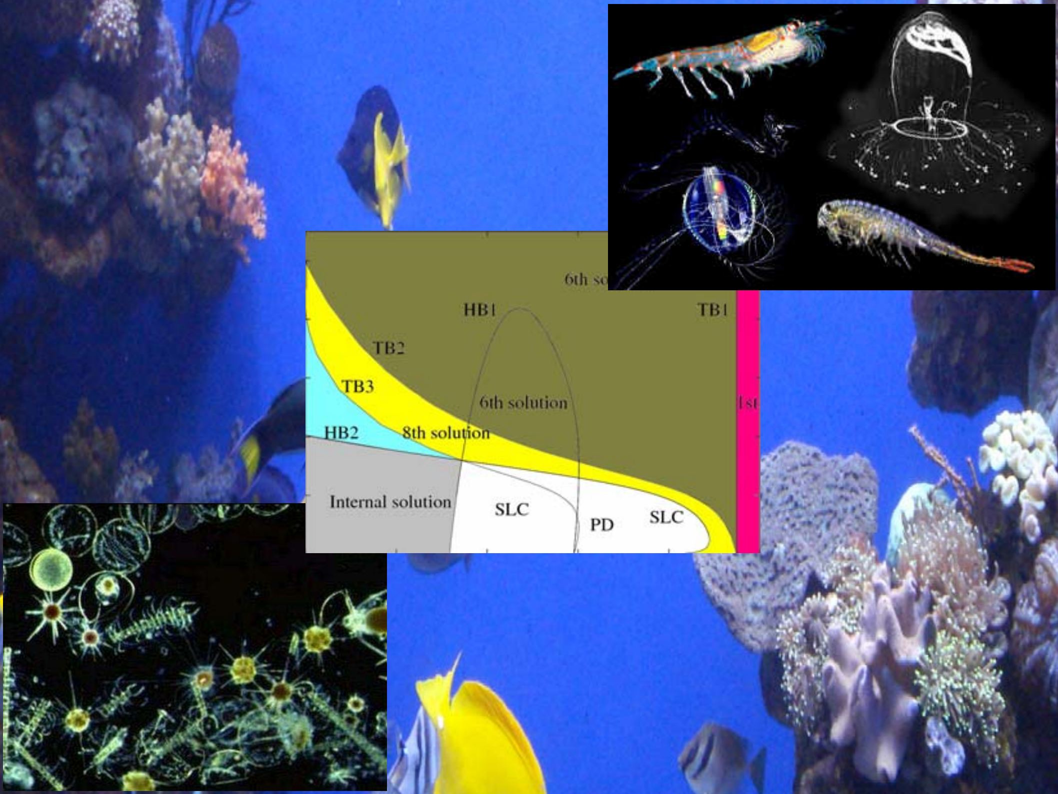

IFISC

Master Thesis

Supervisor: Emilio Hernández-García

UNIVERSITAT DE LES
ILLES BALEARS

Master Thesis

Bifurcation Analysis of a Marine Food Chain

Author:
Flora Souza Bacelar

Supervisor:
Emilio Hernández-García

Instituto de Física Interdisciplinar y Sistemas Complejos

September 9, 2008

Bifurcation Analysis
of a
Marine Food Chain

by

Flora Souza Bacelar

B.S.(Universidade Federal da Bahia) 2001
M.S. (Universidade Federal da Bahia) 2005

THESIS

Presented to

The University of Balearic Islands

in Partial Fulfillment

of the Requirements

for the Degree of

MASTER OF SCIENCE

September 2008

Bifurcation Analysis of a Marine Food Chain

Para meu anjo

André Luis

Que nossos esforços valham a pena !

Acknowledgements

I would like to thank my supervisor for his excellent guidance, our rewarding discussions and his constant feedback and besides to all the IFISC people for proportioning good conferences, seminars, classes and science environment. I also have to thank all my mates for helping me all the time providing me with enjoyable moments.

Gràcies Francesc (Xisco), Rafael, Melchior, Rosario (Xaro) i Catalina (Cati) per donar color i vida al Mateu Orfila.

Um agradecimento especial à toda minha familia (meus tios, tias, primos, amigos...), ao constante apoio e carinho do meu paizinho, minha mamãe e Ruuuuuuuuuuuú e aos que já não estão por aqui, mas que sem dúvida permeiam o espaço celestial apoiando-me sempre. Beijos apertados às minhas saudosas vovós, ao meu vovô e ao meu padrinho Jorge.

Thanks to Roberto, Suani and García for everything and else more. I would like to give my gratitude to my friend Charles, I hope I can help you like you have helped me, thanks and good luck.

A special thanks to my collaborators Josema and Sybille who have contributed to the realization of this work, helping me in the text and giving me insightful suggestions.

I acknowledge support from the European Commission through the integrated project THRESHOLDS (contract 003933) and from MEC (Spain) and FEDER, through project FISICOS (FIS2007-60327) and from *Govern* *de les Illes Balears.*

And finally thank you for opening my master thesis I hope you enjoy reading it as I have enjoyed writing it.

Contents

I Introduction 1

Preface

The application to Biology of the methodologies developed in Physics is attracting an increasing interest from the scientific community. It has led to the emergence of a new interdisciplinary field, called Physical Biology, with the aim of reaching a better understanding of the biological mechanisms at molecular and cellular levels. Statistical Mechanics in particular plays an important role in the development of this new field.

Elements of Physical Biology. Alfred J. Lotka

Last century saw an increasing application of the mathematical methodologies developed in the context of the Physical sciences (differential equation modeling, stability and control concepts, stochastic processes, etc.) to the understanding of biological processes. An early synthesis was provided by the book “Elements of Physical Bilology” authored by Alfred J. Lotka, in particular with results for population dynamics and energetics. The subject grew to a mature stage (see for example the textbook written by Murray, “Mathematical Biology”) and the recent explosive increase in the availability of precise data from living systems has stressed again the need for quantitative approaches to the modeling of cells, organisms and ecosystems.

In this work we analyze with the tools of dynamical systems theory (qualitative and numerical analysis of differential equations, and bifurcation theory) a model for a marine food chain (nutrient, phytoplankton, zooplankton and fish), aiming at considering the join effects of nutrient supply and pollution by a contaminant on the system dynamics.

Marine ecology is the study of marine organisms and their relationship with other organisms and with the surrounding environment, such as non-living, abiotic factors and living, biotic ones. Thus, water, light, temperature, salinity, tides, currents, etc are some of the abiotic factors or physical, chemical and geological elements related to marine areas. The biotic factors compound the interactions among living organisms. One aspect of such interactions can be described through food chains, food network or trophic networks that describe the feeding interactions among species within an ecosystem. Food webs evolve complex network of interactions in contrast with the simple linear pathway of the food chains. Biologists often model food web relationships in terms of the flow of solar energy, captured in photosynthesis by the phytoplankton (primary producers) and passed from organism to organism by means of feeding transfers.

Unfortunately the growing exploitation of biomarine resources, the growing input of nutrients and contaminants due agricultural and industrial activities unbalance the correct functioning and equilibrium of such ecosystems and besides affects the economy of many coastal areas which works with aquaculture, fishing and/or tourism. Because of this and many other reasons, interest and research activity in marine ecology are intensifying which leads to the increasing understanding of the complex interactions evolved in the marine ecosystems.

In the scope of the Thresholds project(*http://www.thresholds-eu.org*) which has the interest focused on regime shifts of ecosystems, the earliest stage of this work consisted of seeking to define a model of food web effects that fit data of the mesocosm experiment carried out in the Isefjord, Denmark for twelve days in 2005. The mesocosm experiment consisted in twelve clear polyethylene cylindrical enclosures that were filled with ambient fjord water to study the combined influences of nutrient enrichment and the pyrene contaminant. With this purpose simplified models were used in order to capture the essential dynamics of mesocosm experiments.

In the attempt to obtain more knowledge of established predator-prey models many analytical and numerical studies were carried out leading to interesting new results and new manner to see these models. Finally the Canale's chemostat model appeared to present the most interesting results and hence the work was split up into two: (i) The present work, that states the behavior of tri-trophic food-chain under an unspecified contaminant and (ii) the work realized by Sibylle Dueri and collaborators, "Modelling the effects of pyrene contamination and enrichment on mesocosm experiments carried out in the Isefjord (Denmark)" that suits the mesocosm data.

In the first chapter the analytical mathematic tools used in this work will be presented. The concepts of the dynamical systems, analysis of stability and bifurcations will be shown in a non-rigorous formalism. Afterwards, some classical and established models of biological growth and interactions of populations will be depicted, in the second chapter.

Finally in the third chapter the joint effect of contaminants and nutrient loading on population dynamics of marine food chains by means of bifurcation analysis will be analyzed. Contaminant toxicity is assumed to alter mortality of some species with a sigmoidal dose-response relationship. A generic effect of pollutants is to delay transitions to complex dynamical states towards higher nutrient load values, but more counterintuitive consequences arising from indirect effects are described. In particular, the top predator seems to be the species more affected by pollutants, even when contaminant is toxic only to lower trophic levels.

Part I

Introduction

1

Dynamical systems: Stability and Bifurcation analysis

Science is built up with facts, as a house is with stones. But a collection of facts is no more a science than a heap of stones is a house.

La Science et l'hypothèse. Poincaré

A system can be defined by a set of interacting elements, in such way there are cause and effect relations in the phenomena that occur to the elements of this set. In a dynamical system some characteristics of the interacting elements change over time. From the Calculus invented by Newton and independently reinvented by Leibniz it is known that the variation of an object (characteristic) $x(t)$ in a continuous time is measured by the derivative $\frac{dx(t)}{dt}$. In this sense the system evolution in time can be described mathematically by [1]:

$$\dot{\vec{x}} = \vec{f}(\vec{x}, \beta) \tag{1.1}$$

Where $\vec{f}$ is the variation rate of the **state variables**, $\vec{x}$, and β is a parameter of the system. When $\vec{f}$ does not depend on time explicitly the system is called **autonomous**. Certain values, $\underset{t\to\infty}{lim}\vec{x}(t) = \vec{x}^*$ with $\vec{f}(\vec{x}^*) = 0$,

---

[1] $\dot{\vec{x}} = \frac{d\vec{x}(t)}{dt}$

do not change over time, depicting a **stationary solution** of equation 1.1, in other words they correspond stagnation (fixed) points of the flow. These **equilibrium** points or fixed points of a system can be classified according with their stability and the topology of their **phase portrait**[2]

1.1 Stability of fixed points

According to Lyapunov, stability is a property of system behavior in neighborhoods of equilibria. When the initial conditions, $\vec{x}(0)$, fit in with a equilibrium point the system remains indefinitely in this point. However, when the initial conditions are inside a sphere of radius δ whose center is a specific equilibrium, $\vec{x}^*$, it can be defined as **asymptotically stable** when all the trajectories, $\vec{x(t)}$, converge to $\vec{x}^*$. If this sphere has a finite radius this point is **locally sable**, otherwise when $\delta \to \infty$ the point is **globally stable**. In both cases the equilibrium point is classified as a **stationary attractor** and all the set of initial conditions that converge to this point form the **basin of attraction** of this attractor.

An equilibrium point is **neutrally stable** when for a sphere of radius δ centered in such point there is another sphere with radius ϵ also centered in $\vec{x}^*$, with $\delta < \epsilon$, such that every trajectory with initial condition inside the sphere of radius δ remains in the second sphere of radius ϵ for al $t \geq 0$. Hence $\vec{x}(t)$ does not tend to $\vec{x}^*$ when $t \to \infty$. When there is at least one trajectory with initial condition belonged to a sphere of radius δ that leaves the sphere of radius ϵ in a finite time the equilibrium is called **unstable**.

All this classification is based on the temporal evolution of the distance between a trajectory $\vec{x}(t)$ and $\vec{x}^*$, for the complicated systems modeled by equation 1.1 that scientists study, explicit solutions for $\vec{x}(t)$ are rarely available. In consequence of this difficulty Lyapunov, [1], developed a method for assessing the conditions of stability indirectly. This method involves

---

[2] Phase portrait, phase space or phase diagram: a plot of the system's trajectories in the state space in which the axes are the state variables. In mechanical systems the phase space usually consists of all possible values of position and momentum(or speed) variables.

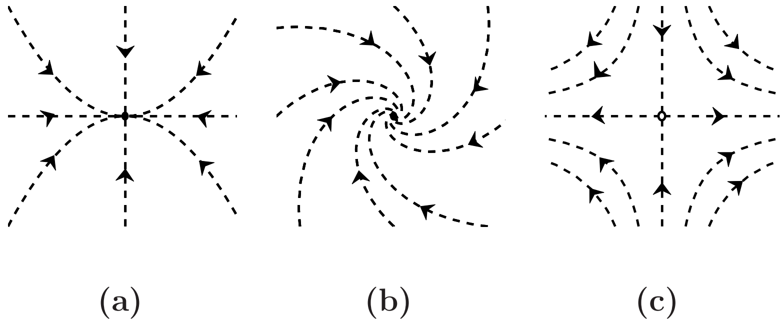

Figure 1.1. Fixed points in two dimensions. (a) Stable Node, (b) Stable Spiral, (c) Saddle Point. The equations that have been used are: (a) $\dot{x} = -0.5x$, $\dot{y} = -y$, (b) $\dot{x} = -x + y$, $\dot{y} = -x - y$, (c) $\dot{x} = x$, $\dot{y} = -y$.

linearizing $\vec{f}$ at $\vec{x}^*$, let **J** be the jacobian matrix of $\vec{f}$ evaluated at $\vec{x}^*$.

$$\mathbf{J} = \frac{\partial \vec{f}(\vec{x}, \beta)}{\partial \vec{x}}\bigg|_{\vec{x}=\vec{x}^*} \tag{1.2}$$

The **eigenvalues** of **J** determine whether $\vec{x}^*$ is stable. These are scalar values λ_i such that [3]$det(\mathbf{J} - \lambda_i \mathbf{I}) = 0$, i.e. the roots of the characteristic polynomial of **J**. In this way, if the eigenvalues are all distinct, it is possible to write a exponential approximation for general solution of the linearized system by:

$$\vec{x}(t) = k_1 \vec{v}_{01} e^{\lambda_1 t} + k_2 \vec{v}_{02} e^{\lambda_2 t} + ... + k_n \vec{v}_{0n} e^{\lambda_n t} \tag{1.3}$$

where n is the dimension of the system, k_i are the arbitrary constants that are given by the initial conditions and the vectors $\vec{v}_{0j}$ are the **eigenvectors** associated with each eigenvalue and are determined by:

$$\mathbf{J}\vec{v_{0i}} = \lambda_i \vec{v_{0i}}, \qquad (i = 1, 2, ..., n) \tag{1.4}$$

Sometimes the Jacobian matrix presents equal real eigenvalues, in this case **multiplicity**[4] of the eigenvalues has to be taken into account in order

---

[3] **I** is the identity Matrix.

[4] The number of equal eigenvalues. If the multiplicity of an eigenvalue is 2, there are two eigenvalues of this same value. If is 3 there are three eigenvalues with this same value and so on.

to generate linearly independent solutions. For example if a two-dimensional system has two equal eigenvalues ($\lambda_1 = \lambda_2 = \lambda$) a general solution for this **degenerate case** is:

$$\vec{x}(t) = k_1\vec{v}_{01}e^{\lambda t} + k_2\vec{v}_{02}\mathbf{t}e^{\lambda t} \tag{1.5}$$

In a n-dimensional case for eigenvalues with multiplicity **m** the associated functions are $e^{\lambda_i t}$, $te^{\lambda_i t}$, $t^2e^{\lambda_i t}$, ..., $t^{m-1}e^{\lambda_i t}$, thus, in the same way as for distinct eigenvalues, the general solution is the linear combination of these functions and the arbitrary constants are determined by the initial conditions.

In two dimensions, according to Poincaré, the fixed points can be classified from the trace $\mathbf{T}$ and the determinant $\mathbf{\Delta}$ of the $\mathbf{J}$ matrix:

- if $\mathbf{\Delta} < 0$, $\lambda_{1,2}$ are real and of opposite signs. The fixed point is called **saddle point** which is unstable in the sense of Lyapunov;
- if $\mathbf{\Delta} > 0$ and $\mathbf{T}^2 - 4\mathbf{\Delta} > 0$, $\lambda_{1,2}$ are real and with the same sign. If $\mathbf{T} > 0$ the point is called a **unstable node**, if $\mathbf{T} < 0$ it will be a **stable node**.
- if $\mathbf{\Delta} > 0$ and $\mathbf{T}^2 - 4\mathbf{\Delta} < 0$, $\lambda_{1,2}$ are complex conjugated. If $\mathbf{T} > 0$ the fixed point is an **unstable spiral**, if $\mathbf{T} < 0$ it is an asymptotic **stable spiral** and if $\mathbf{T} = 0$ the point is a neutrally stable **center**, where the eigenvalues are purely imaginary.

On the line $\mathbf{T}^2 - 4\mathbf{\Delta} = 0$ are lying the **star points** and **degenerate nodes** which are cases where the system presents two equal eigenvalues. In the case of star points, only the main diagonal of $\mathbf{J}$ is different of zero with equal elements, hence the solutions are straight lines passing through x^* in the phase space. If the elements of the diagonal are positive the star is unstable, if the elements of the diagonal are negative the star is asymptotically stable. When $\mathbf{T}^2 = 4\mathbf{\Delta}$ there is a degenerate node that is stable when $\mathbf{T} < 0$ and unstable when $\mathbf{T} > 0$. If $\mathbf{\Delta} = 0$, at least one of the eigenvalues is zero and in this case there is a whole **line** or a **plane of fixed points**. Figure 1.1 shows some of the different mentioned types of fixed points and figure 1.2 depicts the degenerate cases . Hirsch and

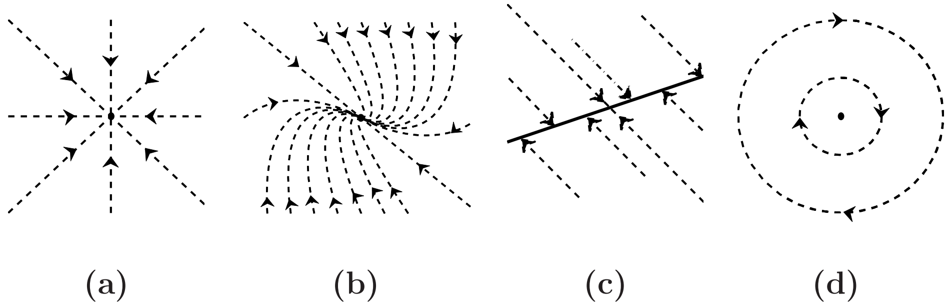

Figure 1.2. Two dimensional degenerate cases of fixed points . (a) Star Node, (b) Degenerate Node, (c) Line of fixed points, (d) Center. The equations that have been used are: (a) $\dot{x} = -x$, $\dot{y} = -y$, (b) $\dot{x} = -x + y$, $\dot{y} = -x - 3y$, (c) $\dot{x} = -x + 3y$, $\dot{y} = x - 3y$, (d) $\dot{x} = y$, $\dot{y} = -x$.

Smale, [2, Chapter 9], give a detailed discussion of stability of fixed points as well as Strogatz, [3, Chapter 5].

Observing the form of the solution 1.3 it can be seen that it converges to stable solution when $Re\lambda_i < 0$ and diverges when at least one eigenvalue λ_i is positive. But in the degenerate cases such as center, star, degenerate node and non-isolated fixed points, the linear system does not guaranty a correct picture of the phase portrait near the fixed point, degenerate points can be altered by small nonlinear terms. In such cases stability must be determined considering non-linear terms of the Taylor series of $\vec{f}(\vec{x}, \beta)$, [3, 4].

As mentioned before the stability of a equilibrium point is established by the sign of the real part of its eigenvalues. Therefore to determine the stability of this solution, taking into account that a fixed point is stable when $Re(\lambda_i) < 0$ for all i, is only necessary to know if the signs of the real parts of λ_i are negative or not. Edward John Routh and Adolf Hurwitz found independently the solution to find out whether all the roots of a polynomial have a negative real part. This criterion of stability known as **Routh-Hurwitz theorem** is very helpful specially when the characteristic polynomial for the eigenvalues of the Jacobian **J** is of order higher than five and it is in general impossible to calculate analytically its roots. The theorem says that the real part of all roots of the polynomial:

$$\lambda^n + a_1\lambda^{n-1} + a_2\lambda^{n-2} + ... + a_{n-1}\lambda + a_n = 0 \tag{1.6}$$

are negative if all the coefficients a_i are positive and if all upper-left determinants $\Delta_i (i = 1, ..., n)$ of the Hurwitz matrix **H** are positive. If the jacobian matrix **J** is $n \times n$ so is **H**. The **H** matrix are made in the following way:

- The coefficients a_i with odd indices and increasing j are written in the first line . In the second line are written the coefficients with even indices and increasing j. Notice that the coefficient of λ^n, a_0, is 1. the other positions are filled up with zeros.
- The two following lines are obtained moving the first two lines one column to the right, filling-in the empty positions with zeros.
- The other lines are built repeating the procedure above until a_n occupies the lower right edge of the matrix.

In this way, for example, for $n = 6$ the Hurwitz matrix is:

$$\mathbf{H} = \begin{pmatrix} a_1 & a_3 & a_5 & 0 & 0 & 0 \\ 1 & a_2 & a_4 & a_6 & 0 & 0 \\ 0 & a_1 & a_3 & a_5 & 0 & 0 \\ 0 & 1 & a_2 & a_4 & a_6 & 0 \\ 0 & 0 & a_1 & a_3 & a_5 & 0 \\ 0 & 0 & 1 & a_2 & a_4 & a_6 \end{pmatrix}$$

and the upper-left determinants $\Delta_i (i = 1, ..., n)$ are:

$$\Delta_1 = |a_1| \ , \ \Delta_2 = \begin{vmatrix} a_1 & a_3 \\ 1 & a_2 \end{vmatrix} \ , \ \Delta_3 = \begin{vmatrix} a_1 & a_3 & a_5 \\ 1 & a_2 & a_4 \\ 0 & a_1 & a_3 \end{vmatrix} \ , \ ... \ , \ \Delta_6 = |\mathbf{H}|$$

In this section it was shown how different sorts of fixed points and their stability characterize the topology of the phase space, see Figures 1.1 and 1.2. When the phase portrait of a dynamical system changes qualitatively its topology as parameters pass through critical values the system suffers a bifurcation that will be explained in the next section.

1.2 Bifurcation analysis

The term bifurcation was introduced by Poincaré, [5], and it is strongly linked to the concept of **structural stability**. In a bifurcation fixed points can be created or destroyed, or their stability can change when varying parameters. When the dynamical system does not change quality of the flow in the phase space under small perturbations of the control parameter the system is structurally stable. In two-dimensional systems there is a theorem that states the necessary conditions for which the system is structurally stable, it is the known **Peixoto's theorem**, see [6].

In this section it will be presented four **local bifurcations** that occur in continuous dynamical systems, such as saddle-node bifurcation, transcritical bifurcation, pitchfork bifurcation and Hopf bifurcation and then the **global bifurcations** homoclinic and heteroclinic. Local bifurcations are those which can be previewed studying the vectorial field in the neighborhood of a fixed point or a closed trajectory. Normally this study is made by through the eigenvalues. Global bifurcations are those which can not be established by a local analysis.

First the **normal forms**[5] of the simplest equilibria bifurcations of codimension one will be depicted. An example of a codimension-two bifurcation will be presented in the ending of this chapter and although this work is not focused on chaos behavior, there are some regions in the bifurcation diagram of the studied system that present chaotic behavior and because of this a period doubling cascade routing to chaos will be briefly explained.

1.2.1 Co-dimension one local bifurcations

Codimension counts the number of control parameters for which fine tuning is necessary to get such a bifurcation, i.e. the smallest dimension of a parameter space which contains the bifurcation in a persistent way. Four local bifurcations can occur varying the values of a unique parameter. The

---

[5] A normal form of a mathematical object is a simplified form of the object obtained by applying a transformation (often a change of coordinates) that is considered to preserve the essential features of the object.

normal form of saddle-node, transcritical and pitchfork bifurcations are given in one-dimensional systems whereas a two-dimensional system is needed for a Hopf bifurcation.

Definition 1.2.1. A dynamical system 1.1 is said to undergo a bifurcation at parameter value $\beta = \beta_0$ if in any (small) neighborhood of $\beta_0 \in \mathbb{R}^m$ there is a β value containing dynamics that are not topologically equivalent to those at β_0.

Saddle-node bifurcation

A saddle-node bifurcation is a local bifurcation in which two fixed points coalesce into a single point that represents a bifurcation point and then this point disappears. The normal form of this bifurcation can be represented in a one-dimensional equation:

$$\dot{x} = \beta - x^2 \tag{1.7}$$

This equation[6] presents two equilibria, for $\dot{x} = 0$, $x^* = \pm\sqrt{\beta}$. When $\beta < 0$ there is no equilibria, when $\beta > 0$ there are two equilibria. Then $\beta = 0$ depicts the transition in the change of flow topology in the phase space, $\beta = 0$ is the bifurcation point, β_0. A way to analyze graphically bifurcations is through the bifurcation diagram, see Figure1.3. But in order to visualize better this bifurcation a two-dimensional equation was plotted , in this case

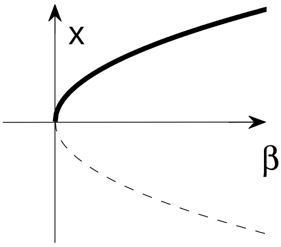

Figure 1.3. Bifurcation diagram: Saddle-node Bifurcation. The thick line is the stable solution and the dashed line is the unstable one.

---

[6] $\dot{x} = \beta + x^2$ is also possible as a normal form of a saddle-node bifurcation.

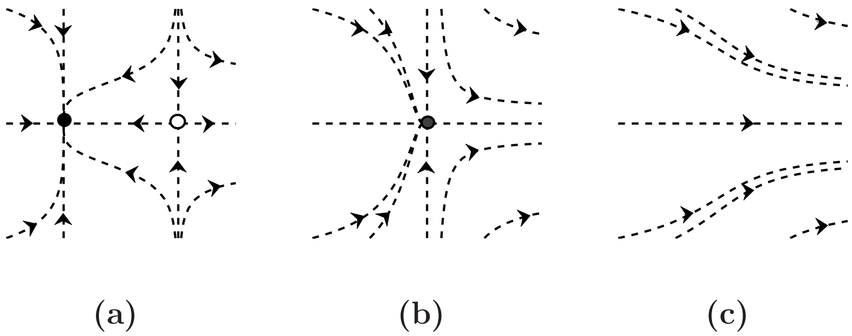

Figure 1.4. Phase space in two dimensions showing a saddle-node bifurcation. (a) $\beta < 0$, (b) $\beta = 0$, (c) $\beta > 0$. The equation that has been used is: (a) $\dot{x} = \beta + x^2$, $\dot{y} = -y$.

it expresses the collision of a stable equilibria (node) with a unstable one (saddle), see Figure1.4.

Transcritical bifurcation

In the transcritical bifurcation, fixed points are not destroyed nor created, but for a critical value of the parameter they switch stability. The normal form of this bifurcation can be:

$$\dot{x} = \beta x - x^2 \tag{1.8}$$

Observe that this equation[7] presents two equilibria, $x^* = 0$ and $x^* = \beta$ and

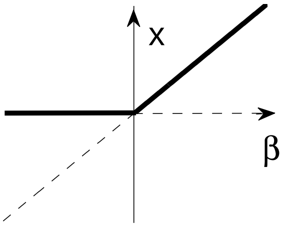

Figure 1.5: Bifurcation diagram: Transcritical Bifurcation

the eigenvalue is given by $\lambda = \beta - 2x^*$. Therefore the fixed point $x^* = 0$ has

---

[7] $\dot{x} = \beta x + x^2$ is also possible as a normal form of a Trancritical bifurcation.

the eigenvalue $\lambda = \beta$ and the fixed point $x^* = \beta$ has the eigenvalue $\lambda = -\beta$ hence in the bifurcation point $\beta_0 = 0$ these point change stability, see Figure 1.5.

Pitchfork bifurcation

A pitchfork bifurcation occurs generically in systems with inversion or reflection symmetry. That is, an equation of motion that remains unchanged if one changes the sign of all phase space variables (or at least for one). This bifurcation has two types: supercritical or subcritical. The normal form of the supercritical pitchfork bifurcation is:

$$\dot{x} = \beta x - x^3 \tag{1.9}$$

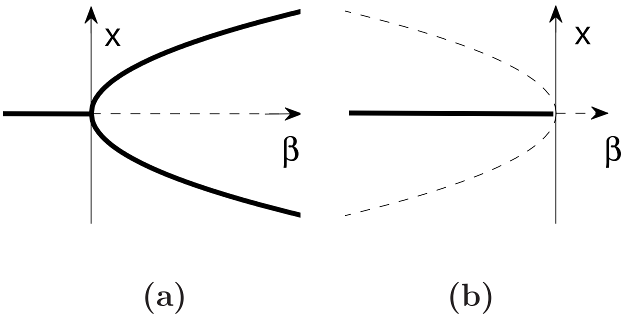

Figure 1.6. Bifurcation diagram: Pitchfork bifurcation . (a) Supercritical, (b) Subcritical.

When $\beta < 0$ there is a stable equilibrium $x^* = 0$ at point $\beta = 0$ this point changes stability and two other equilibria $x^* = \pm\sqrt{\beta}$ appear with the same stability, in this case both are stable. And the normal form for the subcritical case is:

$$\dot{x} = \beta x + x^3 \tag{1.10}$$

In this case, for $\beta < 0$ the equilibrium at $x^* = 0$ is stable, and there are two unstable equilibria at $x^* = \pm\sqrt{-\beta}$. For $\beta > 0$ the equilibrium at $x^* = 0$ is unstable.

Hopf bifurcation

In 1942, E. F. F. Hopf established the conditions in which such bifurcation could occur in a n-dimensional system, [7]. This bifurcation was originally studied by Poincaré, in 1892 [8], and studied by Aleksandr Aleksandrovich Andronov in 1929 for two-dimensional systems, [9]. Because of this sometimes this bifurcation is called Poincaré-Andronov-Hopf bifurcation. A Hopf or Poincaré-Andronov-Hopf bifurcation is a local bifurcation in which a **limit cycle**[8] arises from an equilibrium in dynamical system, when the equilibrium changes stability via a pair of purely imaginary eigenvalues. Like in the Pitchfork bifurcation the Hopf bifurcation has two types: supercritical or subcritical. To obtain this sort of bifurcation minimally a two-dimensional system is demanded. A normal form of Hopf bifurcation could be:

$$\begin{aligned}\dot{x} &= \beta x - y + \sigma x(x^2+y^2), \\ \dot{y} &= x + \beta y + \sigma y(x^2+y^2) \end{aligned} \tag{1.11}$$

This system presents a unique fixed point, the origin ($x^* = 0$, $y^* = 0$). The eigenvalues are $\pm i + \beta$ hence the origin is asymptotically stable for $\beta < 0$ and unstable for $\beta > 0$. For $\beta = 0$ the origin changes stability, if $\sigma = -1$ a **stable limit cycle** arises in the $\beta > 0$ region and in this case the bifurcation is **supercritical**. If $\sigma = 1$ while the origin is stable there is a presence of a **unstable limit cycle** that collapses in the transition of stability of the origin, in this case the bifurcation is **subcritical**. All these facts can be better viewed in the polar coordinates, changing $x = r\cos\theta$ and $y = r\sin\theta$

---

[8] A **limit cycle** is an isolated closed trajectory that can appear in the phase portrait of nonlinear systems. An isolated trajectory means absence of other closed trajectories infinitely close. Therefore the neighboring trajectories must approach or move away from the limit cycle which is a **periodic attractor** or **repeller**. A limit cycle is asymptotically stable when the neighboring trajectories approach the limit cycle otherwise it is unstable. It is important to differentiate limit cycles from closed trajectories surrounding center points. In the last case the closed trajectories are not isolated and there could be several of them infinitely close for close initial conditions. In addition the amplitude, the period and the shape of a limit cycle are determined by the parameters of a nonlinear system while the shape, period and amplitude of closed trajectories surrounding centers depend on the initial conditions.

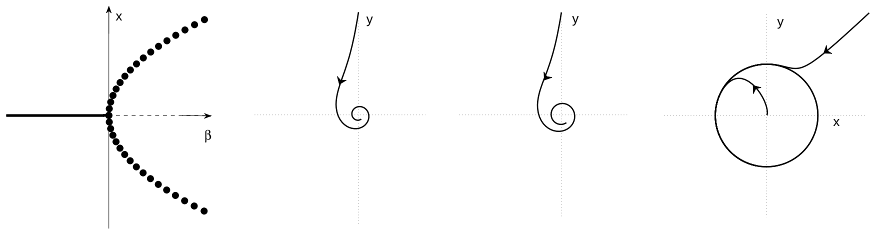

(a) **(b)** **(c)** **(d)**

Figure 1.7. Supercritical Hopf bifurcation ($\sigma = -1$). (a)Bifurcation diagram. Phase space (b) $\beta < 0$, (c) $\beta = 0$, (d) $\beta > 0$.

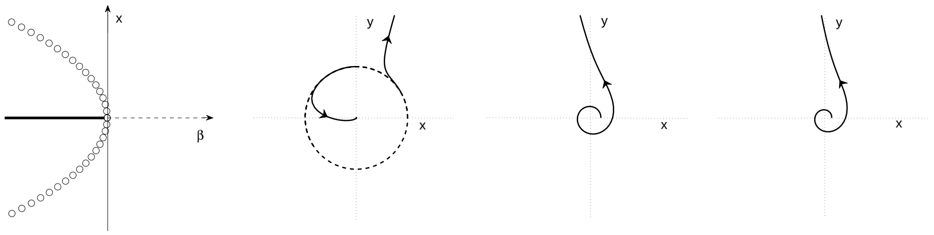

(a) **(b)** **(c)** **(d)**

Figure 1.8. Subcritical Hopf bifurcation ($\sigma = 1$). (a)Bifurcation diagram. Phase space (b) $\beta < 0$, (c) $\beta = 0$, (d) $\beta > 0$.

the system becomes:

$$\begin{aligned} \dot{r} &= h(r) = \beta r + \sigma r^3, \\ \dot{\theta} &= 1 \end{aligned} \tag{1.12}$$

For $\dot{r} = 0$ there are two possibilities, the origin $r^* = 0$ and a cycle with radius $r^* = \sqrt{\frac{-\beta}{\sigma}}$, as stated before when $\sigma = -1$ the eigenvalue in polar coordinates is $\lambda = \frac{dh}{dr}\Big|_{r^*} = \beta - 3(r^*)^2$, analyzing the cycle, for $\beta > 0$, $\lambda = -2\beta$ and hence the limit cycle is stable. If $\sigma = 1$ the eigenvalue is $\lambda = \beta + 3r^2$, for $\beta < 0$, $\lambda = 4\beta$ and hence the limit cycle is unstable. See figures 1.7 and 1.8.

1.2.2 Codimension-one global bifurcations

Global bifurcations can not be previewed by eigenvalues of fixed points, however in 1963 V. D. Melnikov developed a method by which is possible to prove the existence of homoclinic and heteroclinic bifurcations in Hamiltonian perturbed systems, see [10]. In this subsection the homoclinc and heteroclinic bifurcations will be presented briefly .

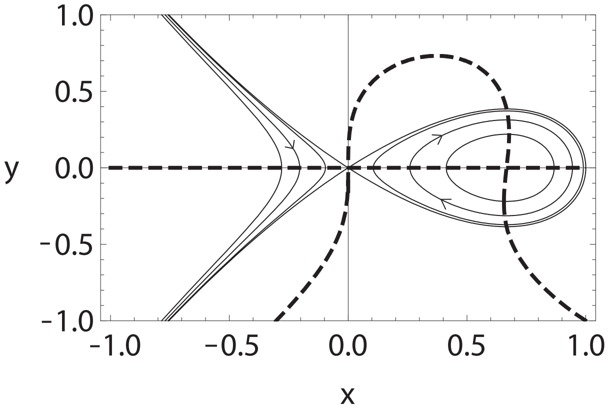

Figure 1.9. Phase space: Homoclinic bifurcation. The limit cycle get close to the saddle point (0,0) when increasing β. The dashed lines are the nullclines for $\beta = -0.1$ and the thick lines are the trajectories ($x^3 - x^2 + y^2 = \beta$) for the increasing values of β, $\beta = -0.1$, $\beta = -0.05$, $\beta = -0.01$ and finally $\beta = 0$ that represents the homoclinic orbit.

Homoclinic Bifurcation

A point is called a **homoclinic point** when it lays down in a trajectory that is, at the same time, a stable and unstable manifold of a saddle point, this trajectory is a **homoclinic orbit**[9]. A bifurcation that leads to a destruction of a of a homoclinic orbit is a **homoclinic bifurcation** . As an example, the following system proposed by Hale and Koçak, [11], presents a homoclinic bifurcation:

$$\begin{aligned} \dot{x} &= 2y \\ \dot{y} &= 2x - 3x^2 - y(x^3 - x^2 + y^2 - \beta) \end{aligned} \tag{1.13}$$

---

[9] Homoclinic trajectory or homoclinic loop

This system presets two fixed points, observe the intersection of the **nullclines**[10] in the Figure 1.9. The origin $(x^* = 0, y^* = 0)$ and the point $(x^* = \frac{2}{3}, y^* = 0)$ are the fixed points of this system. The origin is always a saddle point with eigenvalues $\lambda_i = \frac{1}{2}\left(\beta \pm \sqrt{\beta^2 + 16}\right)$ independently of the values of β. But the point $(\frac{2}{3}, 0)$ changes stability accordingly β varies, its eigenvalue is $\lambda_i = \frac{1}{54}\left(27\beta + 4 \pm \sqrt{729\beta^2 + 216\beta - 11648}\right)$, observe that at $\beta^* = -\frac{4}{27}$ the system suffers a supercritical Hopf bifurcation before which this point is a stable spiral, and than it converts into a unstable spiral. For $-\frac{4}{27} < \beta < 0$ one can see the presence of an orbitally asymptotically periodic orbit, alias limit cycle and at $\beta^* = 0$ the periodic orbit is absorbed by a homoclinic loop, i.e, a homoclinic bifurcation happens, see Figures 1.9 and 1.10, in this case for $\beta > 0$ the homoclinic orbit is destroyed.

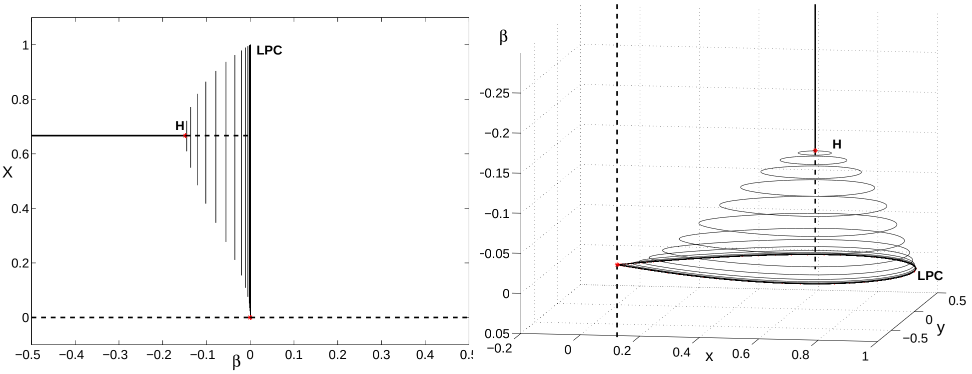

(a) **(b)**

Figure 1.10. Bifurcation diagram: Homoclinic Bifurcation . (a) 2D Bifurcation diagram, (b) 3D Bifurcation diagram. The dashed lines are unstable solutions and thick lines the stable ones.

---

[10] Nullclines or Zero-Growth isoclines of a two-dimensional dynamical system are the boundary between regions where $\dot{x}$ or $\dot{y}$ switch signs. In this way setting either $\dot{x} = 0$ or $\dot{y} = 0$ the nullclines of the system will be found. The intersections between x and y nullclines are the equilibrium points.

Heteroclinic Bifurcation

When the unstable manifold of a steady point becomes the stable manifold of another steady point, thus connecting two steady points, then the system presents a heteroclinic connection, alias **heteroclinic cycle**. A **Heteroclinic bifurcation** happens when the steady points connection is broken. Observe the following system proposed by Hale and Koçak, [11]:

$$\begin{aligned}\dot{x} &= \beta + 2xy \\ \dot{y} &= 1 + x^2 - y^2 \end{aligned} \tag{1.14}$$

In figure 1.11 depicts the phase portrait for three different values of the parameter. At $\beta = 0$ the system presents two fixed points, $(0,1)$ and $(0,-1)$, both of which are saddle points. The orbit in the y-axis between the two points has the stable manifold of $(0,1)$ and the unstable manifold of $(0,-1)$ thus the system has a heteroclinic orbit for $\beta = 0$. For $\beta \neq 0$ the saddle connection is broken hence a heteroclinic bifurcation happens.

1.2.3 Codimension two bifurcations

As mentioned before the number of control parameters necessary to get a bifurcation determined the codimension of this bifurcation. Therefore when two control parameters are necessary to get a bifurcation, such a bifurcation is told to be codimension two. There are several sorts of codimension two bifurcations, such as Bautin, Bogdanov-Takens, Cusp, Fold-Holpf and Hopf-Hopf bifurcations. As an example observe the system that was studied by Takens, [12], and Bogdanov, [13]:

$$\begin{aligned}\dot{x} &= y \\ \dot{y} &= \beta_1 + \beta_2 x - x^2 + xy \end{aligned} \tag{1.15}$$

When $\beta_1 > 0$ there is no equilibrium. For $\beta_1 = 0$ and $\beta_2 = 0$ the origin is the unique equilibrium and its two eigenvalues are zero. For $\beta_1 < 0$ there are two equilibria: $(\sqrt{-\beta_1}, 0)$ and $(-\sqrt{-\beta_1}, 0)$. In this way $\beta_1 = 0$ is a saddle-node bifurcation point. The first fixed point is a saddle with eigenvalues:

$$\lambda_{1,2} = \frac{1}{2}\left(\beta_2 - \sqrt{-\beta_1} \pm \sqrt{\beta_2^2 - 2\sqrt{-\beta_1}\beta_2 - \beta_1 + 8\sqrt{-\beta_1}}\right) \tag{1.16}$$

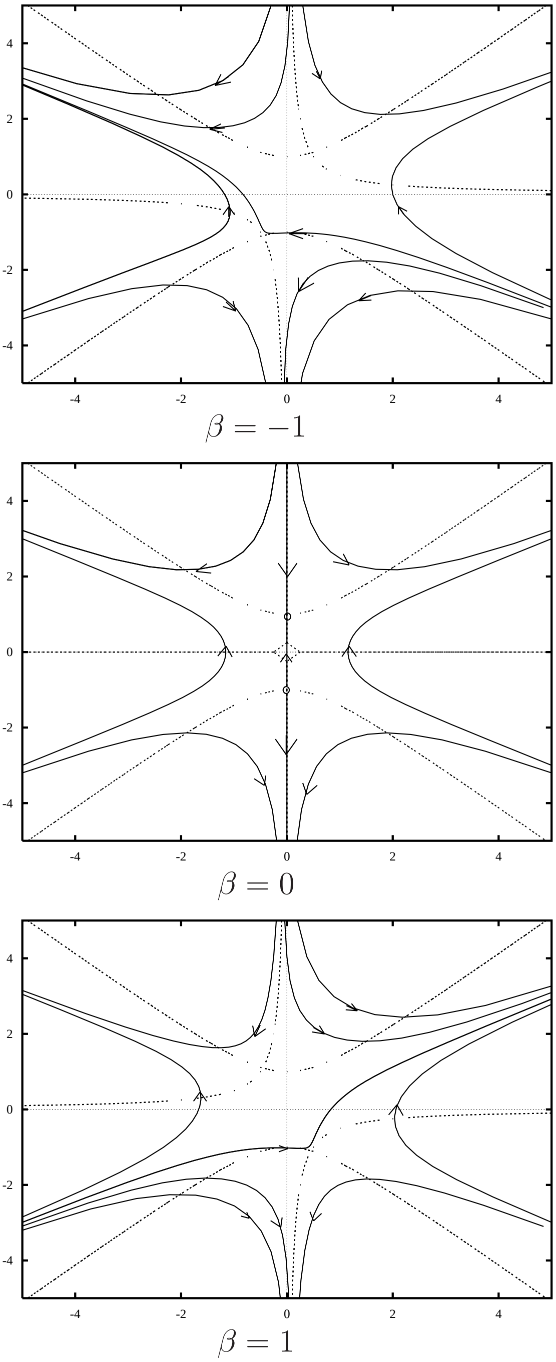

$\beta = -1$

$\beta = 0$

$\beta = 1$

Figure 1.11. Phase space: Heteroclinic Bifurcation. Dashed lines are the nullclines and tick lines are some trajectories.

the second one has the eigenvalues:

$$\lambda_{1,2} = \frac{1}{2}\left(\beta_2 + \sqrt{-\beta_1} \pm \sqrt{\beta_2^2 + 2\sqrt{-\beta_1}\beta_2 - \beta_1 - 8\sqrt{-\beta_1}}\right) \tag{1.17}$$

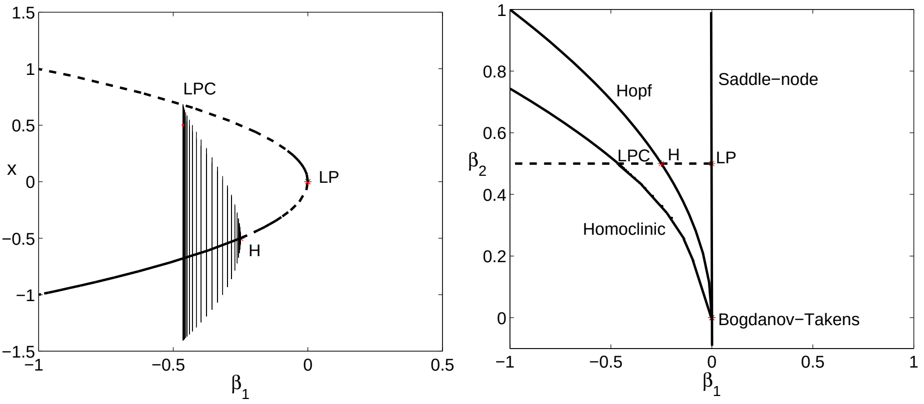

(a) **(b)**

Figure 1.12. Bogdanov-Takens Bifurcation. The first graph is the bifurcation diagram for $\beta_2 = 0.5$. The second one is the two-parameter bifurcation diagram.

For $\beta_2 < -\sqrt{-\beta_1}$ this point is asymptotically stable and unstable for $\beta_2 > -\sqrt{-\beta_1}$. And observing the eigenvalues of the second point one can see that a subcritcal Hopf bifurcation happens at $\beta_2 = -\sqrt{-\beta_1}$, then decresing β_1 from this value on limit cycles arises. Decreasing further more the value of β_1 the cycle is destroyed into a homoclinic bifurcation when it merges with the saddle point, see figure 1.12(a). In the two-parameter graph in figure 1.12(b), it can be seen that a Bogdanov-Takens bifurcation happens. The origin of the parameter plane, coincides with the origin in the cartesian plane and, as mentioned before, this point has two zero eigenvalues and corresponds to the critical value of the **Bogdanov-Takens bifurcation**. Three codimension-one bifurcations occur nearby: a saddle-node bifurcation, a Poincaré-Andronov-Hopf bifurcation and a homoclinic bifurcation.

1.2.4 Period Doubling Cascade and Chaos

Differently to the previous bifurcations a **period doubling** bifurcation or **flip** bifurcation is a local bifurcation related to cycles and has no correspondence for equilibria in continuous systems. In this bifurcation a cycle loses its stability, while another cycle with twice the period of the original cycle rises. If the secondary path is stable the bifurcation is **supercritical** (subtle), conversely, when the secondary path is unstable the bifurcation is **Subcritical** (catastrophic). This bifurcation requires at least a three-dimensional phase space and a supercritical period doubling cascade converges to chaotic behavior. In order to elucidate see the following example.

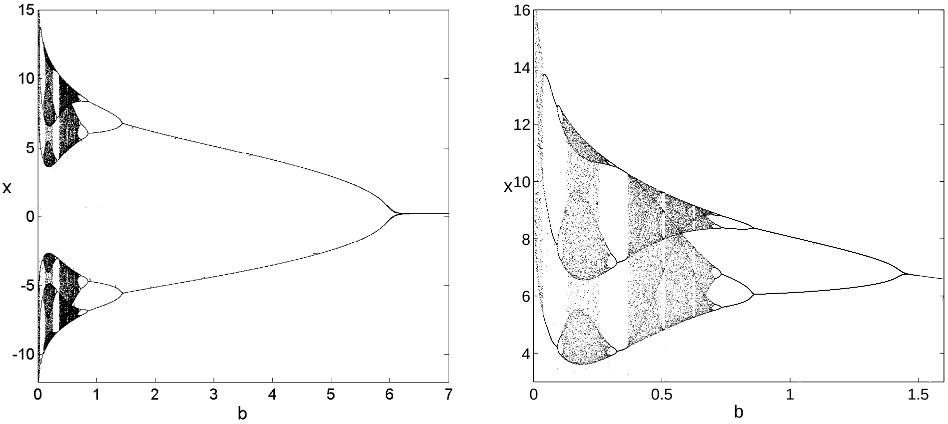

Figure 1.13. Period Doubling Cascade and Chaos for Rössler system, varying b parameter and fixing $a = 0.2$ and $c = 5.7$. The first picture depicts the complete bifurcation diagram, where line between $b = 5.99$ and $b = 7$ is the fixed point that bifurcates in a Hopf bifurcation at b value, 5.99. The other lines represent the maximum and minimum of the cycles. The second picture shows the higher sequence of bifurcations amplified.

Rössler equations

Rössler, [14], proposed the following system in 1976. It is minimal for continuous chaos for at least three reasons: Its phase space has the minimal dimension three, its nonlinearity is minimal because there is a single quadratic

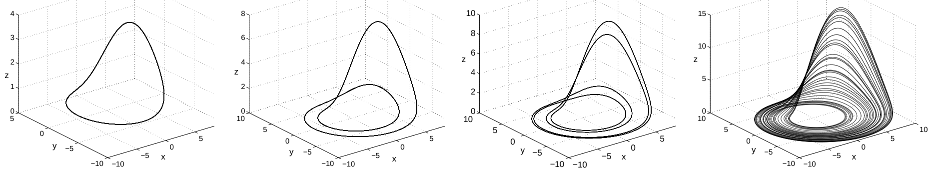

(a) **(b)** **(c)** **(d)**

Figure 1.14. Rössler Phase Space: (a) $b = 2.0$, (b) $b = 1.0$, (c) $b = 0.8$, (d) $b = 0.4$. fixed $a = 0.2$ and $c = 5.7$.

term, and it generates a **chaotic attractor**[11] with a single lobe, in contrast to the Lorenz attractor which has two lobes, [17].

$$\dot{x} = -y - z \tag{1.18}$$

$$\dot{y} = x + ay \tag{1.19}$$

$$\dot{z} = b + z(x - c) \tag{1.20}$$

This system presents stationary, periodic and chaotic attractors depending on the value of the parameters (a, b, c). The figure 1.13 shows the sequence of bifurcations for certain range of parameters, in the first plot a complete bifurcation scenario is plotted, observe that there is a stable fixed point that converts into unstable via a Hopf bifurcation at b value of 5.99 then the stable cycle loses stability through a period doubling bifurcation at a b value of 1.43, another period doubling happen at 0.85 and then at 0.73. Afterwards a cascade of supercritical bifurcations occurs leading to a chaotic attractor, see the last picture of figure 1.14. More information can be also found in the book of Thompson and Stewart, [18, Chapter 12].

The theory of dynamical systems is not an innovation and excellent books have already been published in this issue, specially it's worth citing Strogatz, [3], Hale and Koçak, [11], Thompson and Stewart, [18], Gucken-

---

[11] Also called Strange Attractors, [15]. Actually, in many texts in the literature, the word strange is related to the geometrical structure of attractor, strange attractors are fractals and demonstrate infinite self similarity, while the word chaotic refers to the dynamics of orbits on the attractor. The attractor that will be shown here is a strange chaotic attractor, but it is important to bear in mind, although it will not be shown in this thesis, the existence of **strange nonchaotic attractors**, [16].

heimer and Holmes, [19] and Monteiro, [20, in Portuguese]. The purpose of this chapter is a quick review and a summary of dynamical systems theory. The graphs were drawn using a MATLAB package for numerical bifurcation analysis of ODEs (Matcont), [21], XPPAUT, [22, 23] and my own program codes.

2

Models

Things should be made as simple as possible, but not anymore simpler.

A. Einstein

The previous chapter presented some characteristics and some mathematical analysis of dynamical systems. Here some examples of the simplest biological models will be briefly presented. They still are used to model dynamics of diverse phenomena, such as the various manifestations of populations, social and economic systems and biological organisms.

2.1 Models of growth

Growth is a fundamental property of biological systems, occurring at the level of populations, individual animals and plants, as well as within organisms. Even in technology, growth curves are used to forecast technological performance fitting a set of data and extrapolating the growth curve beyond the range of the data. Much research has been devoted to modeling growth processes, and there are many ways of doing this, including: mechanistic models, time series, stochastic differential equations, etc.

2.1.1 Exponential growth: Malthus Model

The Malthusian growth model, sometimes called the **exponential law of population growth**, [24], describes "*if a population will grow (or decline) exponentially as long as the environment experienced by all individuals in the population remains constant*", [25]. The derivation of a exponential law could be given considering all individuals in the population absolutely identical (in particular, there is no age, sex, size, or genetic structure) and they reproduce continuously. In this way the number of individuals can only change as a result of birth, death, emigration, and immigration. Malthus considered a closed population, without immigration nor emigration, in this approach, the population growth equation can be written as following:

$$\frac{dN}{dt} = (b-d)N \qquad \Rightarrow \qquad N(t) = N_0 e^{(b-d)t} \tag{2.1}$$

where b and d are the birth and death positive rates. If $b > d$ the population grows exponentially, if $b < d$ the population becomes extinct. Exponential growth is only realistic as long as there appears to be no limits to growth. Many systems appear to grow in this fashion for the initial periods until some capacity constraint begins to take place.

2.1.2 Gompertz curve

A model that takes into account capacity constraints is Gompertz's law. In 1825 Gompertz published "On the Nature of the Function Expressive of the Law of Human Mortality", [26], in which he showed that "*if the average exhaustions of a man's power to avoid death were such that at the end of equal infinitely small intervals of time, he lost equal portions of his remaining power to oppose destruction*", [27], then the number of survivors at any age t would be given by the equation:

$$N(t) = ke^{-be^{-ct}} \tag{2.2}$$

where k is the upper asymptote, i.e, the number of individuals in equilibrium, c is the intrinsic growth rate and b, c are positive numbers. Differentiating and taking the logarithm of the **Gompertz equation** 2.2 results the following equations:

$$\begin{aligned} \frac{dN}{dt} &= kcbe^{-ct}e^{-be^{-ct}} = kcN(t)be^{-ct} \\ ln(N) &= ln(k) + ln(e^{-be^{-ct}}) = ln(k) - be^{-ct} \Rightarrow be^{-ct} = ln(k) - ln(N) \end{aligned}$$

combining these two results the Gompertz differential equation becomes:

$$\frac{dN}{dt} = kcN\left(ln(k) - ln(N)\right) \tag{2.3}$$

In other words this model states that, under a given number of individuals, the rate of population increase is positively proportional to the natural logarithm of the number of individuals in equilibrium divided by the given number of individuals. This model was initially used only by actuaries, but recently it has been used as a growth curve in biological and economic phenomena, mobile phone uptake and Internet, [28], population in a confined space and modeling of growth of tumors, [29].

2.1.3 The Pearl-Verhulst logistic equation

Taking the Malthus model and adding a function that describes the concentration of nutrients, C, to limit the production of organisms into the dynamic equations, the following system results:

$$\begin{aligned} \frac{dN}{dt} &= bCN \qquad (2.4) \\ \frac{dC}{dt} &= -\alpha bCN \qquad (2.5) \end{aligned}$$

Performing $\alpha\frac{dN}{dt} + \frac{dC}{dt}$ it is obtained: $\frac{d}{dt}(C - \alpha N) = 0$, thus $(C + \alpha N)(t) = constant = C_0$. In this way $C = C_0 - \alpha N$, substituting this expression in 2.4 and performing some algebraic calculation it results into a single equation called the **logistic equation**:

$$\frac{dN}{dt} = r\left(1 - \frac{N}{K}\right)N \tag{2.6}$$

where the expression $r(1-\frac{N}{K})$ is called an intrinsic growth-speed and K is the carrying capacity, the maximum number of individuals that the environment can support. The logistic equation can be integrated exactly, hence the development of a population, which at initial time $t = 0$ has the size N_0, is:

$$N(t) = \frac{K}{1 + \frac{K-N_0}{N_0} e^{-rt}} \tag{2.7}$$

This equation initially developed for studies of demography by Verhust in 1838, [30], was rediscovered in 1920 by Raymond Pearl and Lowell Reed, [31], who promoted its wide and indiscriminate use.

2.1.4 The chemostat equation

The chemostat is an apparatus in which the growth of microorganisms can be controlled. Basically the system is formed by a nutrient reservoir and a growth chamber, in which the microorganisms reproduce. The name chemostat stands for **chem**ical environment is **stat**ic what means that "*the purpose of the chemostat is to have a quasi-constat microorganism concentration, N, and nutrient concentration, C, allowing a constant rate of harvest*", [32].

Adjusting the equations 2.4 and 2.5, substituting bC in equation 2.4 for $K(C) = K_{max}\frac{C}{K_n+C}$ and introducing the inflow and outflow of nutrients from the reservoir and outflow of harvested microorganisms the following system is obtained:

$$\frac{dN}{dt} = K(C)N - \frac{F}{V}N \tag{2.8}$$

$$\frac{dC}{dt} = -\alpha K(C)N - \frac{F}{V}C + \frac{F}{V}C_0 \tag{2.9}$$

Where $\frac{F}{V}N$ represents flow of the harvested microorganisms, $-\frac{F}{V}C$ corresponds to the outflow and $\frac{F}{V}C$ to the inflow of nutrition. The microorganisms can not reproduce indefinitely because they are not in a chamber of infinite concentration, the function $K(C)$ is the reproduction-rate with upper limit K_{max} and K_n is the concentration at which $K = \frac{1}{2}K_{max}$.

There are still more growth equations discussed in the literature, for instance, by Savageau, [33], and in the articles therein. Each data described by growth equations requires different processes to be considered, in this way many specialized growth equations can be proposed in order to describe different aspects on the dynamics related to the growth. However there are enormous number of examples that are described by these basic growth equations mentioned before and some of these will be used in the last chapter of this thesis.

2.2 Interacting populations models

2.2.1 Lotka-volterra model

In 1925 Alfred Lotka explained deeply the purpose of the new area called **physical biology**, which consists on the application of physical principles in the study of life-bearing systems as a whole in contrast with **biophysics** that treats the physics of individual life processes. Among some examples employed in this area he proposed a model to describe chemical reactions in which the concentrations oscillates, [34]. One year hence, using the same equations, different studies were carried out by Vito Volterra, [35]. The main purpose of his work was to describe the observed variations in some species of fish in the Upper Adriatic sea. The system of equations proposed by Lotka and Volterra describes the change of prey or host density with time, and assumed, for this purpose, that the number attacked per predator was directly proportional to prey density. This model became known as **Lotka-volterra predator-prey equations**:

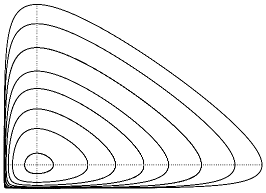

Figure 2.1. LOTKA-VOLTERRA: THE PURELY PERIODIC SOLUTIONS.

$$\frac{dN_1}{dt} = r_1 N_1 - \alpha N_1 N_2 \qquad (2.10)$$

$$\frac{dN_2}{dt} = \delta\alpha N_1 N_2 - d_2 N_2 \qquad (2.11)$$

Where N_1 is the density of prey, N_2 is the density of predator, r_1 is growth rate of prey, d_2 is the mortality rate of predator, α is the predation rate coefficient and δ is the reproduction rate of predators per 1 prey eaten (predation efficiency). This model generates **neutral stability**, see figure 2.1, but the "*assumptions are very unrealistic since very few components are included, there are no explicit lags or spatial elements, and thresholds, limits, and nonlinearity are missing*", [36].

The rate at which prey are taken by predators is known as the **functional response**, depending on the behavior of both the predator and the prey. A remarkable variety of functions has been proposed to characterize the functional response. In the classical Lotka-Volterra model this rate is the product αN_1 in equation 2.10, other functional responses are going to be shown in the next subsection. **Numerical response** is defined in different ways, however, the numerical response is usually modeled as a simple multiple of the functional response, so the numerical response assumes the same shape as the functional response like $\delta\alpha N_1$ in equation 2.11.

2.2.2 Holling types of predation

One improvement of Lotka-Volterra model is to add the logistic growth of prey and besides change the type of predation, functional response, into a more realistic forms. Holling in his article "The functional Response of Predators to Prey Density and its Role in Mimicry and Population Regulation", [37], reviewed previous papers, [38, 39], and analyzed a series of data of invertebrates and vertebrates species. Basically he presented three different types of predation functional responses, P, Holling types:

- Type I: Linear, the number of prey consumed per predator is assumed to be directly proportional to prey density until a saturation value after which it remains constant, so initially the fuctional response is the same used in the Lotka-Volterra model until saturation. This functional response is found in passive predators like spiders.

$$\begin{aligned} P &= \alpha N_1 N_2, \quad if\ N_1 < N_T \\ P &= \alpha N_T N_2, \quad if\ N_1 > N_T \end{aligned} \tag{2.12}$$

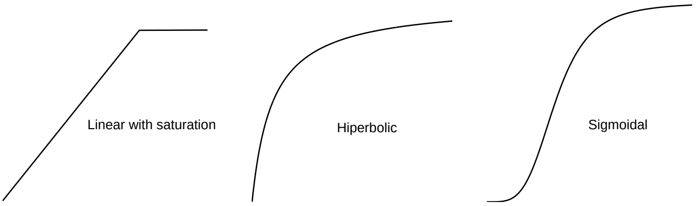

Figure 2.2: Holling Types. (a) Type I, (b) Type II, (c) Type III.

- Type II: hyperbolic functional response in which the attack rate increases at a decreasing rate with prey density until it becomes constant at satiation. This response is typical of predators that specialize on one or a few prey.
$$P = \alpha \frac{N_1}{h + N_1} N_2 \tag{2.13}$$
- Type III: S-Shape or Sigmoidal, this functional response occurs in predators which increase their search activity with increasing prey density showing a initial S-shaped rise up to a constant maximum consumption.
$$P = \alpha \frac{N_1^2}{h^2 + N_1^2} N_2 \tag{2.14}$$

α represents the rate of successful search (predation rate coefficient) and h is the half saturation of the function, see figure 2.2. Basically in these three types only two variables affecting predation were considered, prey and predator density. They were considered by Crawford Stanley Holling in his article of 1959, [38], to be the only essential ones, against other characteristics that were considered not to be essential, such as characteristics of the prey (e.g., reactions to predators, stimulus detected by predator, etc), density and quality of alternate foods available for the predator and characteristics of the predator (e.g., food preferences, efficiency of attack, etc). When such complex interactions are involved, it is difficult to understand clearly the principles involved in predation in this instance a simplified situation was taken into account where some of the variables are constant or not operating.

Without more explanations it is worth citing other sort of predations functional responses in the literature:

- Gause in his book " The struggle for existence", [40], proposed a model that explained the behavior of predator-prey system embodied by Didiniurn-Paramecium. For large density of predator, N_2, its mortality is negligible for positive values of prey density, $N_1 > 0$. In addition, the increase of predator only slightly depends on N_1. To reduce the dependence upon N_1 the term N_1, used in the Lotka-volterra model, was substituted by $\sqrt{N_1}$ in the predation functional response.

$$P = \alpha N_1^{\frac{1}{2}} N_2 \tag{2.15}$$

- Rosenzweig generalized the expression proposed by Gause taking N_1 to the gth power $0 < g \leqslant 1$, [41].

$$P = \alpha N_1^g N_2, \quad 0 < g \leqslant 1 \tag{2.16}$$

- Watt proposed another non-linear connection between the relative increase of the predator and the number of prey, [42].

$$P = \alpha (1 - e^{-aN_1}) N_2 \tag{2.17}$$

2.2.3 Rosenzweig: Paradox of Enrichment

"*Instability should often be the result of nutritional enrichment in two-species interactions*", [41]. Rosenzweig showed for six different predator-prey models that increasing the food supply in the system can lead to destruction of the food species that are wanted in greater abundance, the enrichment was taken increasing the prey carrying capacity and he showed that for a threshold value the steady state is destroyed while a limit cycle rises. This process was called the **paradox of enrichment**.

2.2.4 Kolmogorov general model

Kolmogorov in 1936 studied predator-prey models of the general form:

$$\begin{aligned} \frac{dN_1}{dt} &= N_1 \quad g(N_1, N_2) \\ \frac{dN_2}{dt} &= N_2 \quad h(N_1, N_2) \end{aligned} \tag{2.18}$$

where g en h are continuous functions of N_1 and N_2, with continuous first derivatives. This model was reviewed by May in 1972, [43], who proved that limit cycle behavior is implicit in essentially all conventional predator-prey models. This model requires density dependence or resource-limitation effects at least for the prey population in contrast with the original Lotka-Volterra model which invokes exponential population growth. These sort of nonlinear two-dimensional equations possess either a stable equilibrium point or a stable limit cycle, a fact that can be guaranteed by the **Poincar-Bendixson theorem**, [43]. In three dimensional systems, [20], there are two more possible attractors such as torus, [44] and strange attractors.

Part II

Original Research

3

Joint effects of nutrients and contaminants on the dynamics of a food chain in marine ecosystems

3.1 Introduction

Marine waters and in particular coastal waters are increasingly exposed to anthropogenic pressures represented not only by the growing input of nutrient and contaminants related to urban, agricultural and industrial activities, but also by the exploitation of coastal areas for aquaculture, fishing and tourism. Since the resources of the coastal zone are exploited by different stakeholders it is essential to improve the knowledge on the ecosystem's vulnerability to stressors and protect those areas through a sensible management.

The interaction of pollutants and nutrients on aquatic ecosystems is difficult to evaluate, since many direct and indirect effects have to be considered. Contaminants can have instantaneous effects, such as massive killings after an accidental contaminant release. Other toxic effects, such as genotoxicity and reproductive failure are less evident and they act on a longer time-scale; however, they represent an important risk for the ecosystem. Furthermore, if the contaminant is lipophilic[1], bioaccumulation[2] should be considered. On the other hand, an increase of the nutrient load can have the direct effect of raising the primary production at the bottom of the food chain and consequently increase the concentration of the organic matter in the system. But the higher concentration of organic matter can affect the bioavailability of the contaminants and therefore the fate of pollutants in the aquatic environment and their effects on the impacted ecosystem [45].

Thus, contaminants affect aquatic ecosystems through direct and indirect effects [46], from acute and/or chronic toxicity on sensitive species to disruption in the food web structure. Some species might be more sensitive than others to a certain chemical, but since the different populations are linked to each other by competition and predation, species which are not directly stressed may respond indirectly [46]. Within a food web, community-level relations arise from unobservable indirect pathways. These relations may give rise to indirectly mediated relations, mutualism and competition [47]. In some cases environmental perturbations alter substantially the dynamics or the structure of coastal ecosystems and the effect may produce the occurrence of a trophic cascade and eventually the extinction of some species [48]. A better understanding of the relative importance of top-down (e.g. overfishing) versus bottom-up (e.g. increased nutrient input causing eutrophication) controls is essential and can only be achieved through modelling [49].

Sudden regime shifts and ecosystem collapses are likely to occur in stressed ecosystems. Catastrophic regime shifts have been related to alternative stable states which can be linked to a critical threshold in such a way that a gradual increase of one driver has little influence until a certain value is reached at which a large shift occurs that is difficult to reverse [50, 51]. The shape of ecotoxicological[3] dose-response curves [52], showing a sharp increase in the effect of toxic substances above a critical value, facilitates the occurrence of regime shifts under pollutant pressure.

---

[1] The ability of a chemical compound to dissolve in fats, oils, lipids.

[2] An increase in the concentration of a chemical in a biological organism over time.

[3] "The branch of toxicology concerned with the study of toxic effects, caused by natural or synthetic pollutants, to the constituents of ecosystems, animal (including human), vegetable and microbial, in an integral context."

This study considered the combined effects of contaminant substances and nutrient load in the framework of a simple tritrophic food chain model. The study was restricted to contaminants, such as s-triazines[4], which affect the mortality in particular trophic levels, but which do not bioaccumulate neither in time nor along the food chain. When studying the dynamics of simple food chain and food web models it is also important to bear in mind that the response might depend on the complexity of the represented system. Chaotic dynamics, for example, seems to be more frequent in simple ecosystem models or in models with a high number of trophic levels [53]. Thus, only the first qualitative changes of behavior occurring when increasing nutrients from low values, and how this is changed by pollutants, will be focused. And not the complex sequences of chaotic states which may occur at high nutrient availability, whose details are more affected by the trophic structure of the model.

Since no microbial recycling loop was included, sediment or oxygen dynamics, or shading effects, complex eutrophication behavior typical of coastal ecosystems [54], e.g. anoxic crises, alteration of nutrient cycling, macroalgal blooms, etc. will not occur in the model. The study was rather concentrated in the simplest scenarios occurring during enrichment and its modification by contaminants, discussing particularly the indirect effects which lead to counterintuitive behavior.

3.2 Model formulation

The Canale's chemostat model (CC) was considered, [55, 56, 57], which is an extension of the tri-trophic food-chain Rosenzweig-MacArthur model (RMA) that has been extensively studied in theoretical ecology [58, 59, 60, 61, 62, 63, 64, 65]. This model was previously used to analyze the dynamics of a food chain consisting of bacteria living on glucose, ciliates and carnivorous ciliates [56, 57], but can be adapted to represent an aquatic food chain with

---

[4] s-triazine is one of three organic chemicals, isomeric with each other, whose empirical formula is $C_3H_3N_3$. The three isomers of triazine are distinguished from each other by the positions of their nitrogen atoms, and are referred to as 1,2,3-triazine, 1,2,4-triazine, and 1,3,5-triazine or s-triazine. Among other usages triazine is used in the manufacture of resins and as the basis for various herbicides.

a constant nutrient input. The CC model is similar to the RMA model, but there is an additional equation representing the input of nutrient and it considers the losses due to the flushing rate:

$$\begin{aligned}
\dot{N} &= D(I-N) - P\frac{a_1 N}{b_1+N}, && (3.1)\\
\dot{P} &= P\left[e_1\frac{a_1 N}{b_1+N} - \frac{a_2 P}{b_2+P} - d_1 - f_1 D\right], && (3.2)\\
\dot{Z} &= Z\left[e_2\frac{a_2 P}{b_2+P} - \frac{a_3 F}{b_3+Z} - d_2 - f_2 D\right], && (3.3)\\
\dot{F} &= F\left[e_3\frac{a_3 Z}{b_3+Z} - d_3 - f_3 D\right]. && (3.4)
\end{aligned}$$

In this study the variables N, P, Z, F represent the nitrogen concentration in the different compartments of the system (nutrient, phytoplankton, zooplankton and fish, which will be also denoted with the alternative names of nutrient, prey, predator, and top-predator, respectively) expressed in units of mgN/l. The default parameters, see Table 3.1, were derived from the parameters of the aquatic food chain model presented in [66] and from the pelagic ecosystem model in [67]. I is the nutrient load or nutrient input into the system. D is a flow rate quantifying water renewal in the system, which affects the species through the flushing rates f_i $(i = 1, 2, 3)$. d_i are the specific mortalities, b_i half saturation constants for the Holling type-II predation functions, a_i are maximum predation rates, and e_i efficiencies. The following condition should be satisfied by the equation parameters:

$$e_i a_i > d_i + Df_i \quad (i = 1, 2, 3), \tag{3.5}$$

since this “avoids the case where predator and top-predator cannot survive, even when their food is infinitely abundant” [68]. Contaminant toxicity is incorporated in the model by an increase in mortality. Three different scenarios were considered in each of which the contaminant affects the mortality of only one of the compartments:

$$d_j = d_j^{(0)} + \Delta d_j \left(\frac{(C_j)^6}{(C_j)^6 + 0.5^6}\right) \tag{3.6}$$

Table 3.1: Parameters of the CC model.

Parameters		value	Units
Nutrient input	I	0.15	mg N/l
Inflow/outflow rate	D	0.02	day^{-1}
Max predation rate	a_1	1.00	day^{-1}
	a_2	0.50	day^{-1}
	a_3	0.047	day^{-1}
Half saturation cont	b_1	0.008	mg N/l
	b_2	0.01	mg N/l
	b_3	0.015	mg N/l
Efficiency	e_1	1.00	-
	e_2	1.00	-
	e_3	1.00	-
Mortality(base values)	d_1	0.10	day^{-1}
	d_2	0.10	day^{-1}
	d_3	0.015	day^{-1}
Flushing rate	f_1	0.01	day^{-1}
	f_2	0.01	day^{-1}
	f_3	0.01	day^{-1}

$j = 1, 2$, and 3 labels the three trophic levels: prey, predator and top-predator, C_j is the dimensionless concentration of the contaminant affecting the level j, normalized in such a way that for $C_j = 0.5$ the toxicity achieves half its maximum impact on mortality, and a sigmoidal function (Fig. 3.1) has been used to model the mortality increase from a baseline value, $d_j^{(0)}$, to the maximum mortality, $d_j^{(0)} + \Delta d_j$, attained at large contaminant concentrations. This represents typically the shape of the dose-response curves found when assessing toxic effects of chemical on biological populations [52]. Other works that have studied bifurcations due to mortality changes in the CC model [20] have normally considered a linear increase. The values of $d_j^{(0)}$ and Δd_j used are written in Table 3.2.

3.3 Steady states

This system presents the following set of fixed points: The nutrient-only state (Nu):

$$\begin{aligned} N &= I, \\ P &= 0, \\ Z &= 0, \\ F &= 0. \end{aligned} \tag{3.7}$$

The nutrient-phytoplankton state (NP):

$$\begin{aligned} N &= \frac{b_1(d_1 + Df_1)}{a_1e_1 - d_1 - Df_1}, \\ P &= \frac{De_1\left(\frac{b_1(d_1+Df_1)}{a_1e_1-d_1-Df_1} + I\right)}{d_1 + Df_1}, \\ Z &= 0, \\ F &= 0. \end{aligned} \tag{3.8}$$

There are two solutions (NPZ) characterized by the absence of the top

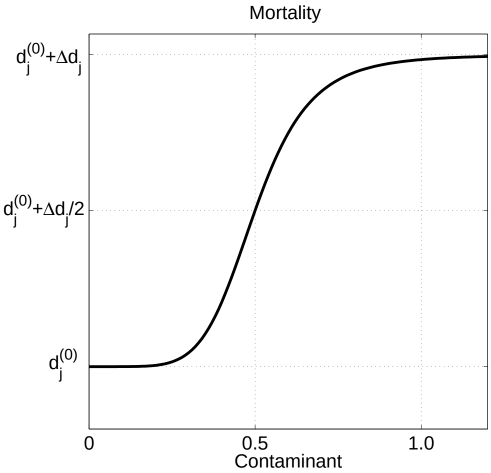

Figure 3.1. Sigmoidal response of mortality to the concentration of the toxic contaminant, according to Eq. (6).

Table 3.2: Contaminant parameters for the three compartments, $j = 1, 2, 3$.

j	$d_j^{(0)}$	Δd_j
1 (prey)	0.1	0.5
2 (predator)	0.1	0.3
3 (top-predator)	0.015	0.015

predator:

$$\begin{aligned}
N &= \frac{b_1D + a_1P - DI \pm \sqrt{4b_1D^2I + (-b_1D - a_1P + DI)^2}}{2D}, \\
P &= \frac{b_2(d_2 + Df_2)}{a_2e_2 - d_2 - Df_2}, \\
Z &= -\frac{(b_1d_1 + b_1Df_1 + d_1N - a_1e_1N + Df_1N)(b_2 + P)}{a_2(b_1 + N)}, \\
F &= 0.
\end{aligned} \tag{3.9}$$

but only the one with the positive sign of the square root is positive definite.

And finally there are three internal fixed points (NPZF), in which all species are alive. From the equation for $\dot{N}$, (3.1), an equation for P as a function of N is obtained. Introducing it into (3.2) together with the expression for $Z = \bar{Z}$ which is obtained from (3.4), the following equation for N is obtained:

$$[A_1N^3 + A_2N^2 + A_3N + A_4] = 0 \tag{3.10}$$

where

$$\begin{aligned}
A_1 &= D(a_1e_1 - d_1 - D_0f_1), \\
A_2 &= -a_1^2b_2e_1 - D(d_1 + Df_1)(2b_1 - I) + a_1(b_1De_1 + b_2(d_1 + Df_1) + a_2\bar{Z} - De_1I), \\
A_3 &= b_1(-D(d_1 + Df_1)(b_1 - 2I) + a_1(b_2(d_1 + Df_1) + a_2\bar{Z} - De_1I)), \\
A_4 &= b_1^2D(d_1 + Df_1I).
\end{aligned} \tag{3.11}$$

The values of the remaining variables at the three internal fixed point solutions can be written in terms of $\bar{Z}$ and of the three values of $N = \bar{N}$ obtained from the cubic 3.10:

$$\begin{aligned}
N &= \bar{N}, \\
P &= D_0(I - \bar{N})\frac{b_1 + \bar{N}}{a_1\bar{N}}, \\
Z &= \bar{Z} = \frac{b_3(d_3 + Df_3)}{a_3e_3 - d_3 - Df_3}, \\
F &= \frac{(a_2e_2P - b_2d_2 - b_2Df_2 - d_2P - Df_2P)(b_3 + \bar{Z})}{a_3(b_2 + P)}.
\end{aligned} \tag{3.12}$$

It turns out that only one of the three fixed point solutions is positive for the parameter values in Table 3.1.

Mathematically there are four additional solutions but they are not feasible biologically since they lead to negative populations: the state characterized by the absence of phytoplankton ($N = I, P = 0, Z \neq 0, F \neq 0$), by the absence of nutrient and of the top-predator ($N = 0, P \neq 0, Z \neq 0, F = 0$), by the absence of the nutrient and of phytoplankton ($N = 0, P = 0, Z \neq 0, F \neq 0$), and by the absence of nutrient ($N = 0, P \neq 0, Z \neq 0, F \neq 0$).

3.4 Stability and bifurcation analysis

The dynamics of the CC food-chain models has been analyzed for several parameter values by direct numerical integration of the model equations, and by bifurcation analysis carried on with the software XPPAUT, [22, 23]. Background on the different types of bifurcations can be found in [3, 19]. Only bifurcations of positive solutions were considered and, as stated in the introduction, the routes to chaotic behavior occurring at high nutrient loadwere not described in detail. For low and intermediate nutrient load the relevant attractors are the fixed points described above, and also two limit cycles, one involving the variables N, P and Z, lying on the $F = 0$ hyperplane, and another one in which all the species are present. These attractors are represented in Fig.3.2.

3.4.1 The non-contaminant case

First, system behavior for the case of mortalities at their base values was considered, i.e. in the absence of contaminants. This will serve as a reference for later inclusion of contaminants. Fig.3.3 shows the sequence of bifurcations when increasing the nutrient input I. For very low input, only nutrients are present in the system (solution (3.7)). When $I > I^{TB1}$, with

$$I^{TB1} = \frac{b_1(d_1 + Df_1)}{a_1 e_1 - d_1 - Df_1} , \tag{3.13}$$

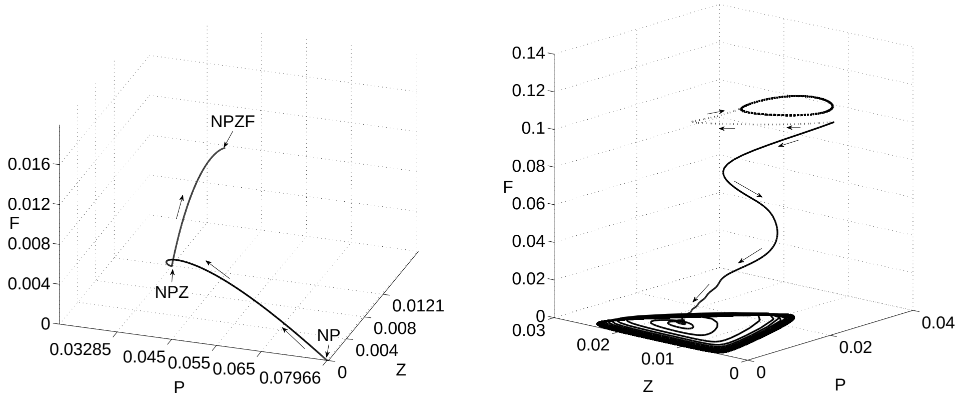

Figure 3.2. a) Projection on the PZF subspace of a trajectory which starts close to the NP fixed point, approaches the NPZ one, and finally is attracted by the NPZF fixed point. $I = 0.4\ mgN/l$, $C_1 = C_3 = 0$, and $C_2 = 0.8$. This shows the approximate location of these points and that only the NPZF one is stable for these parameter values. (b) Cyclic behavior: Thick line is a trajectory leading to an attracting limit cycle on the NPZ hyperplane for $I = 0.1\ mgN/l$, $C_1 = C_2 = 0$, and $C_3 = 0.8$; dotted line is a trajectory attracted by the limit cycle involving all the variables for $I = 0.24\ mgN/l$, $C_1 = C_2 = 0$, and $C_3 = 0.2$.

phytoplankton becomes positive in a transcritical bifurcation (which was called TB1) at which the NP state (3.8) becomes stable. Since $I^{TB1} = 0.0008909$ is very small, this bifurcation can not be clearly seen in Fig. 3.3. From this value on, further enrichment leads to a linear increase of phytoplankton (3.8), until a second transcritical bifurcation, TB2, at which zooplankton becomes positive and the NPZ solution (3.9) becomes stable. It happens at

$$I^{TB2} = \frac{(d_1 + Df_1)(P^{NPZ}d_1 - P^{NPZ}a_1e_1 - b_1De_1 + P^{NPZ}Df_1)}{De_1(d_1 - a_1e_1 + Df_1)} \qquad (3.14)$$

where P^{NPZ} is the expression for P in the NPZ solution, (3.9). From this point the zooplankton starts increasing (keeping phytoplankton concentration at a constant value) until a new bifurcation TB3 occurs, at which the fish concentration starts to grow from zero while zooplankton remains constant, phytoplankton increases, and nutrients decrease (this is the positive interior solution NPZF, Eq. (3.12)). The value of I^{TB3} is given implicitly by:

$$d_3^{TB3} = \frac{Z^{NPZ} a_3 e_3 - Z^{NPZ} D f_3 - b_3 D f_3}{Z^{NPZ} + b_3} \tag{3.15}$$

where Z^{NPZ} is the expression for Z in the NPZ solution, (3.9).

One of the first counterintuitive indirect effects present in the food-chain dynamics has been noticed here: In the NPZF solution, increase of nutrient leads to decrease in nutrient concentration (see Fig. 3.3). The reason is the top-down control that the higher predator begins to impose on zooplankton, leading to positive and negative regulation on the compartments situated one or two trophic levels below Z, respectively.

Shortly after becoming unstable at TB3, the fixed point NPZ experiences a Hopf bifurcation (HB1) which leads to a limit cycle on the NPZ hyperplane. Since the whole hyperplane has become unstable before this bifurcation occurs, this cycle has no direct impact on long time dynamics, although it can affect transients, and it will become relevant when adding contaminants. The steady coexistence of the three species at the NPZF fixed point remains stable until a new Hopf bifurcation HB2 occurs at which the fixed point becomes unstable and oscillations involving the three species and the nutrients (Fig. 3.2) occur. The instabilization of steady coexistence by the appearance of oscillations, which could facilitate extinctions if the amplitude of oscillation is sufficiently large, is the well known “paradox of enrichment”, first mathematically described by Rosenzweig [41]. A good overview of the studies connected with this issue can be found in the paper [69]. See also [70, 71, 72, 73].

Gragnani et al. [64] demonstrated that the dynamics of Canale’s model for increasing nutrient supply is qualitatively similar to the one of the RMA model. After the stationary and cyclic states described above, chaotic behavior followed a different cyclic behavior with higher frequency are found. Also, the maximal average density of top-predator is attained at the edge between chaotic and high frequency cyclic behavior. It was not further described these states but the concentration was in the modifications arising from toxic effects of contaminants on the dynamics, for small and moderate nutrient loading.

3.4.2 Contaminant toxic to phytoplankton

Now the contaminant C_1 is introduced. It increases the mortality of phytoplankton according to expression (3.6) for $i = 1$. Expressions for the bifurcation lines TB1, TB2 and TB3 as a function of I and C_1 can be obtained simply by replacing the mortality (3.6) into the corresponding expressions (3.13), (3.14), and (3.15), respectively. The same can be done numerically for the Hopf bifurcation lines HB1 and HB2. The result is shown in the 2-parameter bifurcation diagram of Fig. 3.4.

Because of the sigmoidal effect of the contaminant (3.6), its impact is mild for $C_1 \ll 0.5$, and it will saturate for $C_1 \gg 1$. Thus, in both limits the bifurcation lines become parallel to the horizontal axis. The interesting behavior is for intermediate values of C_1, where the bifurcation lines are displaced towards higher values of I. That is, the first effect of the contaminant is to stabilize the simplest solutions, the ones stable at lower nutrient load, delaying until higher nutrient loads the transitions to the most complex ones.

But this stabilizing effect is different for the different solutions, and the most important qualitative change occurs at point M in Fig.3.4. It is a codimension-2 point at which the transcritical bifurcation TB3, involving the NPZ and the NPZF fixed points, and the Hopf bifurcation HB1 of the NPZ point, meet. A new Hopf bifurcation line of the NPZF equilibrium, HB3, emerges also from that point. The cycle created at HB3 consists in oscillations of all the four variables, similarly to the cycle created at HB2. Other characteristics of the organizing center M is that the Hopf bifurcations change subcritical to supercritical character across it, and also that a line (not shown) of saddle-node bifurcations of the cycles created at HB1 and HB3 emerges also from M. There are a number of additional structures in parameter space emerging from double-Hopf points, and transcritical bifurcations of cycles which were not described further here.

Despite the complexity of the above scenario, its effect on the bifurcation sequence when increasing nutrient level (up to moderate levels) in the presence of contaminant values beyond M is rather simple (see Fig.3.5): since the lines TB3 and HB1 have interchanged order, the Hopf bifurcation HB1 in which a stable limit cycle is created in the hyperplane $F = 0$ occurs before the appearance of a positive NPZF equilibrium. As a consequence, fish remains absent from the system even at relatively high nutrient levels. This is one of the counterintuitive outcomes of indirect effects: adding a substance which is toxic for phytoplankton makes fish to disappear, whereas the oscillating phytoplankton levels are indeed comparable with the ones at zero contaminant (see Fig. 3.5). As in the absence of contaminant, period doubling and transition to chaos, which have not been analyzed in detail, occur when increasing further the value of I.

A different view of the transitions can be given by describing the bifurcations occurring by increasing the contaminant concentration at constant I. Fig. 3.6 shows that for an intermediate value of the nutrient load, $I = 0.15\ mgN/l$. The NPZF fixed point is stable at low contaminant, but oscillations appear when crossing the HB3 lines. Very shortly after that, this limit cycle involving all species approaches the $F = 0$ hyperplane until colliding with the cycle lying on that plane, which involves only the N, P, and Z species. At this transcritical bifurcation, this limit cycle from which fish is absent becomes stable and is the observed solution for larger C_1. As before, adding a substance which is toxic for the bottom of the trophic chain has the main effect of suppressing the top-predator.

3.4.3 Contaminant toxic to zooplankton

As before, the mortality expression (3.6) for $j = 2$ can be inserted in the expressions (analytical or numerical) for the bifurcations TB1, TB2, TB3, HB1, and HB2 to elucidate the impact of the contaminant C_2, acting on zooplankton, into the food chain dynamics. As in the C_1 case, the bifurcation lines become displaced to higher nutrient load values, so that the sequence of bifurcations of Fig. 3.3 becomes delayed to higher values of I. This is seen in the 2-parameter bifurcation diagram of Fig. 3.7. At difference with the C_1 case, the TB3 and HB1 lines do not cross, so that there are no further qualitative changes with respect to the case without contaminants (Fig. 3.3), at least up to moderate values of I.

Another view of the consequences of Fig. 3.7 can be seen in Fig. 3.8, which shows the different regimes attained at a fixed intermediate value of I ($I = 0.15\ mgN/l$) and increasing C_2. The most remarkable indirect effect is that, for $C_2 < C_2^{TB3} = 0.5103$, zooplankton remains constant despite the increase of C_2 which is toxic to it. The net effect of C_2 in this range is to decrease the amount of fish until extinction. Only for $C_2 > C_2^{TB3}$ contaminant kills zooplankton until extinction at $C_2 = C_2^{TB2} = 0.7406$.

3.4.4 Contaminant toxic to fish

The simplest bifurcation lines are shown in Fig. 3.9 as a function of I and C_3, the contaminant affecting fish mortality. As in the cases before, bifurcations are delayed to higher values of I when contaminant is present. As in the C_1 case, this delay is different for the different lines, resulting in a crossing of TB3 and HB1 in a codimension-2 point M, joining there also a new Hopf bifurcation HB3 of the NPZF fixed point and other bifurcation lines (not shown). Additional structures emerging from other codimension-2 points, such as double-Hopf points are also presented but they were not studied in detail. The qualitative behavior when increasing I at large C_3 (Fig. 3.10) is similar to the C_1 case: there is a succession of N, NP and NPZ fixed points followed by a Hopf bifurcation which leads to oscillations of the N, P and Z variables, remaining the fish absent from the system. Only at relatively high nutrient values does the NPZF steady state become stable at the subcritical branch of the Hopf bifurcation HB3 before becoming unstable again at HB2. Two of the NPZF internal solutions (3.12) which, in contrast with the $C_3 = 0$ case, are positive here, collide at a limit point. In Fig. 3.9 the line of these points as a function of the I and C_3 parameters is labelled as LP. The two solutions exist above that line, and cease to exist below. The sequence of bifurcations encountered when increasing C_3 at constant intermediate values of I is also similar to the C_1 case of Fig. 3.6 in that the NPZF stable fixed point becomes a cycle involving all the variables when HB3 is crossed, and in that this falls onto the $F = 0$ plane shortly afterwards. The details of the last transition, however, are somehow more complex.

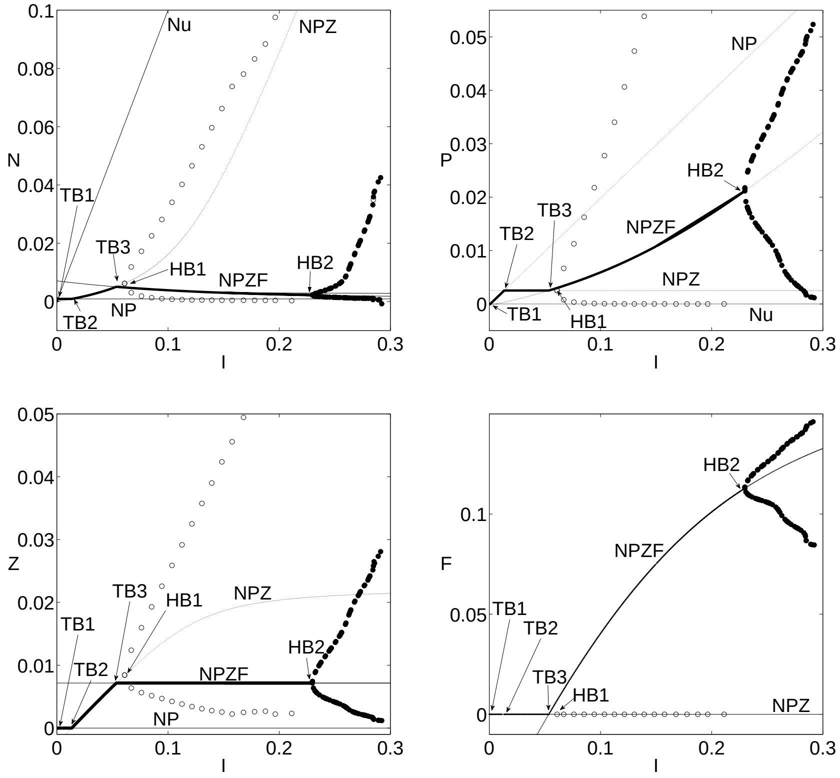

Figure 3.3. Bifurcation diagrams of the four variables as a function of nutrient input parameter I. Thick lines and full symbols denote stable fixed points and maxima and minima of stable cycles, respectively, and thin lines and open symbols, unstable ones. The name of the fixed points is indicated. The relevant bifurcations (described in the main text) occur at $I^{TB1} = 0.0008909\ mgN/l$, $I^{TB2} = 0.01345\ mgN/l$, $I^{TB3} = 0.05352\ mgN/l$, $I^{HB1} = 0.06101\ mgN/l$, and $I^{HB2} = 0.2298\ mgN/l$, locations which are indicated by arrows.

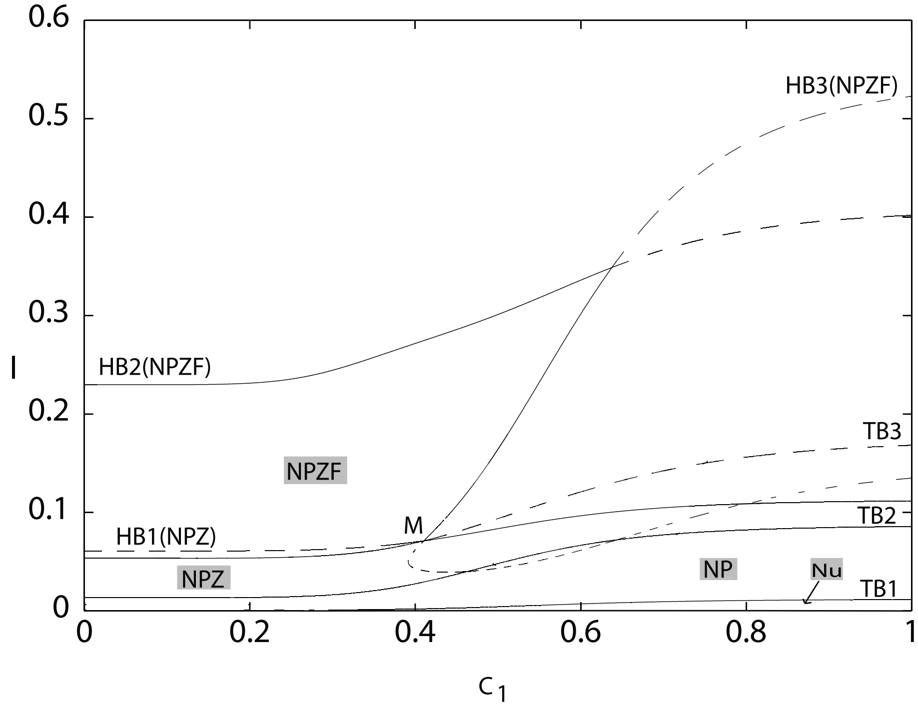

Figure 3.4. Some of the bifurcations occurring as a function of nutrient input I and contaminant C_1 affecting phytoplankton. The name of the bifurcation lines is indicated (for the case of the Hopf lines HB1, HB2 and HB3, the name of the fixed point involved in the bifurcation is shown in parenthesis). Crossing the continuous lines involves a qualitative change for the state attained by the system. Inside regions surrounded by continuous lines, the name of the relevant stable fixed point is shown inside grey squares. Crossing the discontinuous bifurcation lines does not involve a change in the stable state (because, e.g., they correspond to bifurcations of already unstable states). Immediately above the HB2 line, a limit cycle involving all the species is the relevant attractor for low values of C_1. The limit cycle on the $F = 0$ hyperplane is the relevant attractor above the HB1 line for large C_1. Additional bifurcations (not shown) occur in other regions of the open areas above HB1 and HB2.

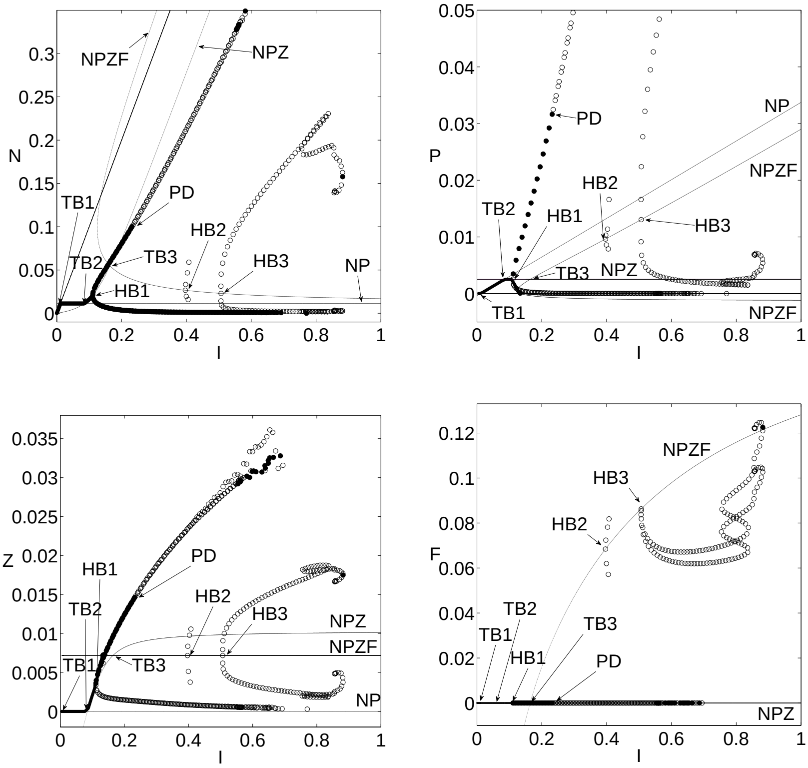

Figure 3.5. Bifurcation diagrams of the four variables as a function of nutrient input parameter I, at a constant high value of the contaminant affecting phytoplankton, $C_1 = 0.9$. Thick lines and full symbols denote stable fixed points and maxima and minima of stable cycles, respectively, and thin lines and open symbols, unstable ones. The name of the fixed points is shown. The bifurcation points are identified by arrows. PD is a period doubling bifurcation.

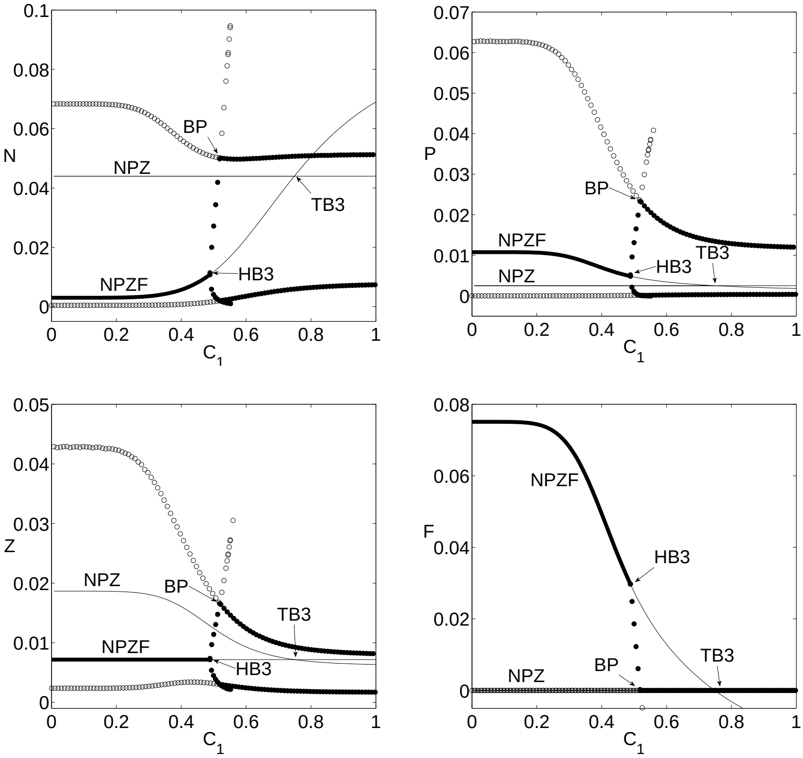

Figure 3.6. Bifurcation diagrams of the four variables as a function of C_1, at constant nutrient input $I = 0.15$ mgN/l. Thick lines and full symbols denote stable fixed points and maxima and minima of stable cycles, respectively, and thin lines and open symbols, unstable ones. BP is a transcritical bifurcation of cycles. The name of the fixed points is shown. The bifurcation points are identified by arrows.

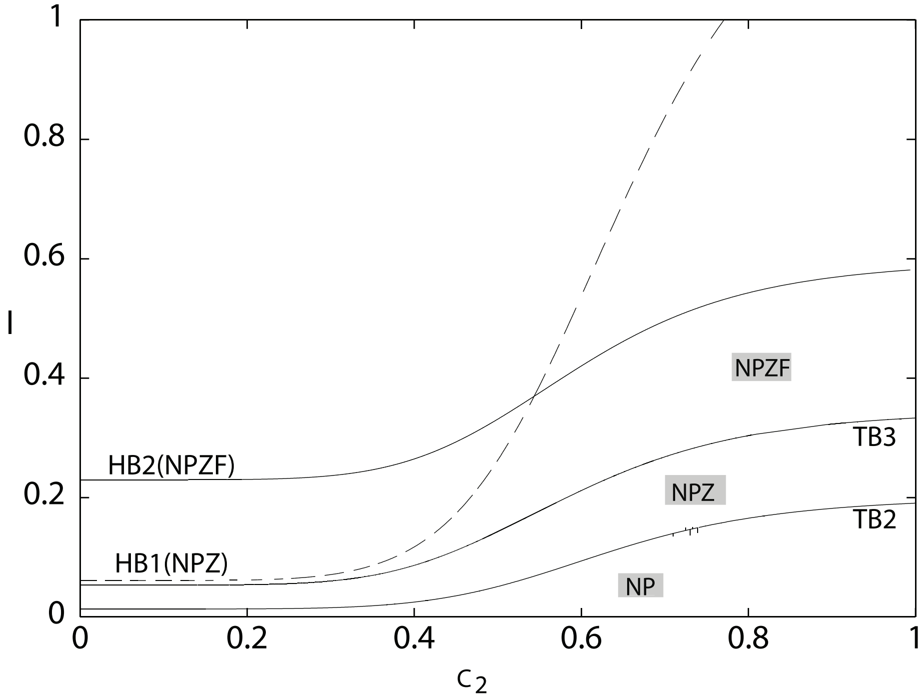

Figure 3.7. Some of the bifurcations occurring as a function of nutrient input I and contaminant C_2 affecting zooplankton. Names of fixed points and bifurcation lines as in Fig. 3.4, as well as the meaning of continuous and discontinuous lines. Immediately above the HB2 line, the relevant attractor is a limit cycle involving all the species. Additional bifurcations (not shown) occur at higher values of I.

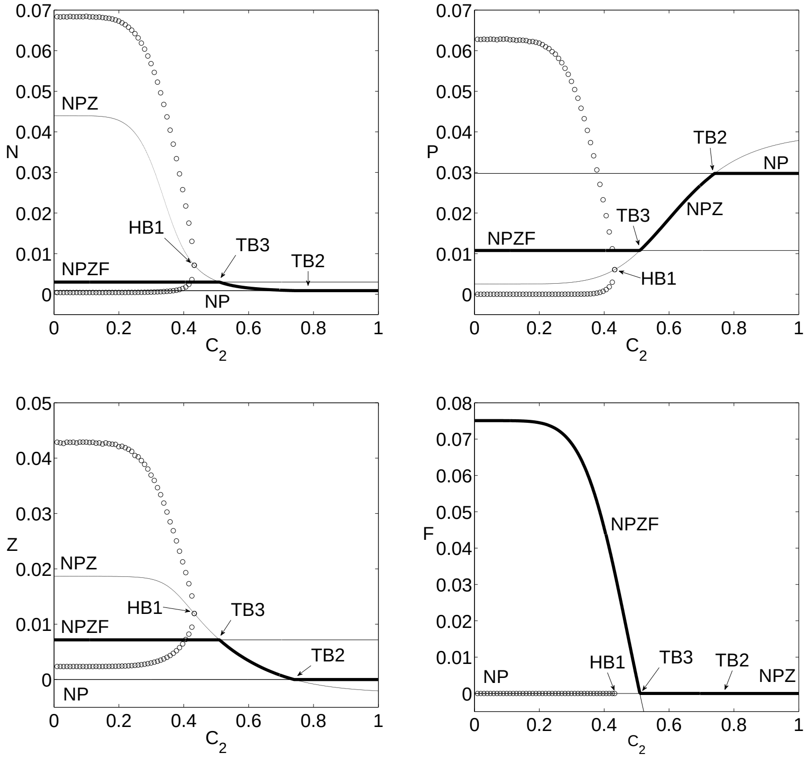

Figure 3.8. Bifurcation diagrams of the four variables as a function of C_2, for a constant nutrient load $I = 0.15\ mgN/l$. Thick lines denote stable fixed and thin lines and open symbols, unstable fixed points and maxima and minima of unstable cycles. The name of the fixed points is shown. The bifurcation points are identified by arrows.

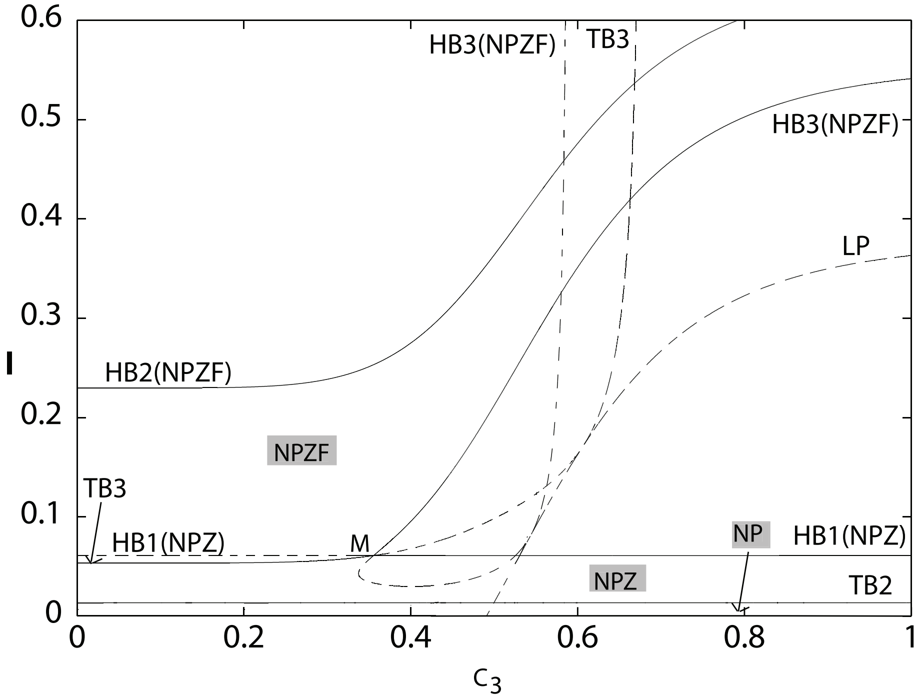

Figure 3.9. Some of the bifurcations occurring as a function of nutrient input I and contaminant C_3 affecting fish. Names of fixed points and bifurcation lines as in Fig. 3.4, as well as the meaning of continuous and discontinuous lines. Immediately above the HB2 line, the relevant attractor is a limit cycle involving all the species. Additional bifurcations (not shown) occur at higher values of I. There is a region of the area labelled as NPZF in which this stable fixed point coexists with a stable limit cycle on the $F = 0$ hyperplane.

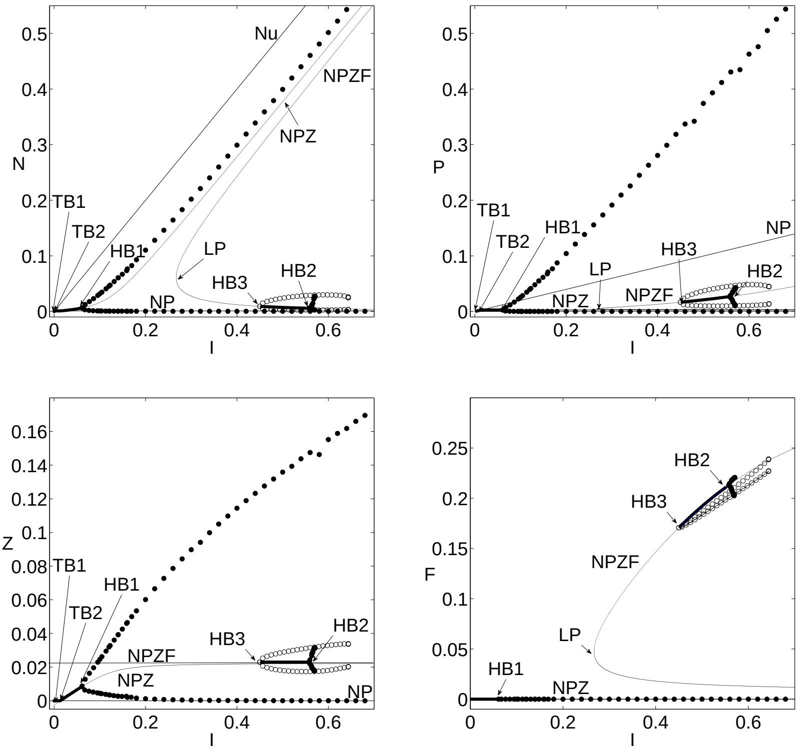

Figure 3.10. Bifurcation diagrams of the four variables as a function of nutrient input rate parameter I for a high value of the contaminant affecting fish, $C_3 = 0.7$. Thick lines and full symbols denote stable fixed points and maxima and minima of stable cycles, respectively, and thin lines and open symbols, unstable ones. The name of the fixed points is shown. The bifurcation points are identified by arrows. There is a small region of coexistence (between HB3 and HB2) of the stable NPZF fixed point and a stable limit cycle on the $F = 0$ hyperplane, which leads later to coexistence of two limit cycles.

4

Discussion and conclusion

We have seen that, because of the assumed sigmoidal influence of contaminant on mortality, toxic effects on our food chain model have a distinct effect at low and at large concentrations, with rather fast transition behaviour in between.

At small and moderate contaminant concentrations the main effect is a displacement of the different bifurcations towards higher nutrient load values, so that transitions to states containing less active compartments, and states without oscillations, become relatively stabilized. Contaminants increase the stability of the food chain with respect to oscillations caused by increased nutrient input. A similar outcome has been observed in [74] for a food-chain model composed of a toxin producing phytoplankton, zooplankton and fish population. In that study chaotic dynamics can be stabilized by increasing the strength of toxic substance in the system.

For higher contaminant values, in most of the cases there is a reordering of the different transitions, giving rise to the appearance of new bifurcations which change qualitatively the sequence of states encountered by increasing nutrient input. The main effect, even in the cases in which such reordering does not occur (the case of C_2 contaminant), is that the top predator becomes the most depleted, being even brought to extinction. This strong impact of the contaminant on the higher predator occurs even in the cases in which the direct toxic effect is on lower trophic levels. It seems that the increased mortality at lower trophic levels becomes nearly compensated by a debilitation of top-down control exerted by higher predators. Obviously, the top predator can not benefit from this mechanism, thus becoming the most affected.

Extrapolation of the above findings for real ecosystems may be problematic, because of the much higher food web complexity found in nature. We believe however that the counterintuitive indirect effects described above should be kept in mind when analyzing the complex responses that ecosystems display to changes in external drivers such as nutrient load and pollutants, and that the detailed identification of them performed here can help to interpret some aspects of the behaviour of real ecosystems.

A

Numerical continuation Programs

A.1 XPPAUT

Although there is a good explanation how you can use XPPAUT to continue your equations in the webpage *http://www.math.pitt.edu/ bard/xpp/xpp.html*, a breath explanation to start using AUTO from XPP will be given in this appendix. Besides some tips in order to help you to get rid of some trick problems. In the home page cited before you can download the XPPAUT program and follow the instructions how to install it.

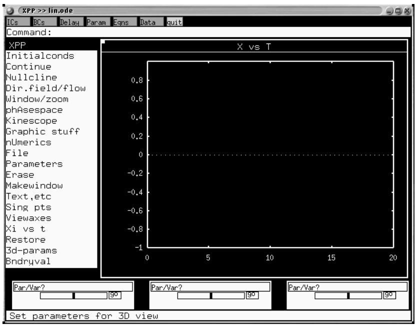

Figure A.1: XPP window.

XPP is a freely available tool written in C-language for solving differential equations, difference equations, delay equations, functional equations, boundary value problems, and stochastic equations. Besides, it contains the code for the popular bifurcation program, AUTO, [22]. It can be used in the following platforms: Linux, MacOs, Unix and Windows.

Before start using XPPAUT you have to write your system into a **ode** file. In this file you have to write the system to be studied, the initial conditions, the parameter values and , if you want, some numerical specifications, such as the time step size, the amount of time to integrate, the parameter range and tolerance error in the algorithm used. Observe the following example of an ode file.

```
# RMA model
dX1/dt=X1*(R*(1-X1/K)-A2*X2/(B2+X1))
dX2/dt=X2*(E2*A2*X1/(B2+X1)-A3*X3/(B3+X2)-D2)
dX3/dt=X3*(E3*A3*X2/(B3+X2)-D3)

# D3=0.015+0.015*cont^6+h^6

#The initial condition
#par D2=0.01,D3=0.005
X1(0)=0.181022
X2(0)=0.0333333
X3(0)=1.65108

#D2=0.01,D3=0.015
X1(0)=0.0939155
X2(0)=0.128571
X3(0)=1.57478

#The parameters
par D2=0.01,D3=0.015
par R=0.5,K=0.2
par A2=0.4,B2=0.1,E2=1
#par h=0.5,cont=0
par A3=0.05,B3=0.3,E3=1

#The XPP options
@ total=2000, bounds=1000
@ Nmax=2000, Ds=0.005,Dsmin=0.001
@ EPSL=1e-06,Dsmax=0.01,EPSU=1e-06,EPSS=1e-06
@ ParMin=0, ParMax=0.3
```

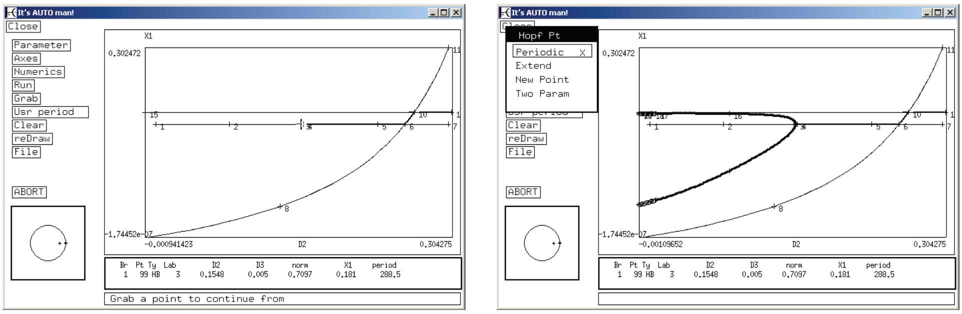

```
Br  Pt Ty  Lab     D2      D3     norm     X1     period
 1   99 HB   3   0.1548   0.005   0.7097   0.181   288.5
Grab a point to continue from
```

```
Br  Pt Ty  Lab     D2      D3     norm     X1     period
 1   99 HB   3   0.1548   0.005   0.7097   0.181   288.5
```

Figure A.2. Auto window: Bifurcation Diagram showing fixed points and periodic solutions.

```
@ Xmin=0,Ymin=0
@ Xmax=1,Ymax=1

done
```

Bifurcation analysis must be started from either a fixed point or a periodic orbit. Sometimes, there are complicated parameter zones in which AUTO calculation is too slow or does not converge. To solve this kind of numerical complications i) you can reduce the tolerances (EPSL, EPSS, EPSU) that present the default value 10^{-4}, but usually the better value of the tolerances is 10^{-7} or ii) you can start from another fixed point value in order to scape from the complicated zone of parameters. In the ode file example you can observe two set of initial conditions, the set of initial conditions considered by XPP will be the last one you write, regarding parameters, AUTO considers the first parameter written as the one to continue the solutions. But you can change the parameters as well as the numerical specifications in the XPP menu without changing your ode file.

XPP can be used to calculate fixed points and then the result can be written in your ode file to avoid calculating it again. To continue a fixed point, go to the AUTO window : click on “Run” and then on “Steady state”. Using the system of equations cited in the example you will find the bifurcation diagram like in the first picture of Figure A.2. To follow periodic solutions, you grab a HP point that designates a Hopf bifurcation and click on “Run” and select “Periodic” as shown in the second picture of Figure

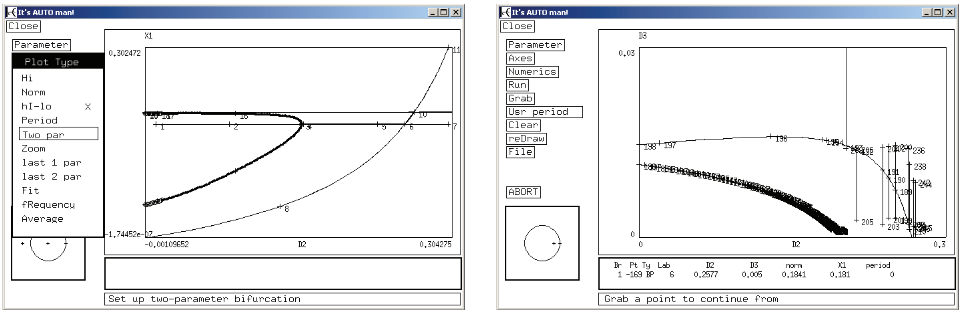

```
Set up two-parameter bifurcation
```

```
 Br  Pt Ty  Lab        D2        D3       norm        X1     period
  1 -169 BP    6     0.2577     0.005     0.1841     0.181         0
```

```
Grab a point to continue from
```

Figure A.3: Two-parameter bifurcation Diagram.

A.2 and a branch of periodic solutions will appear.

In order to analyze changes in the phase portrait of the system when varying two parameters you have to select "Axes" then "Two parameters" and a window will appear to select the main parameter and the second parameter. You can never start continuations from two parameter calculus, first you have to continue from one parameter and afterwards grab the special points to study two-parameter curves. As the same situation with starting points, problems with convergence and speed of calculus can occur, in this way the main and second parameter can be switched to obtain complete two-parameter curves, see Figure A.3.

The AUTO window is not convenient to edit the plot. Consequently the postscript is generated without any possibilities of change except by using a postscript editor afterwards. However, from the AUTO window you can save the bifurcation diagram data which can be used later to make nicer figures using XPP or another software. Recently it was posted on the XPP's webpage a link to a worthwhile Matlab function that orders the messy diagram outputs of XPPAUT and generates graph which can be modified using the graph tools of Matlab. But I've made my own Matlab program to solve some plotting problems when there are "MX" points, that means failure to converge. Figure A.4 shows some plots of AUTO data using Matlab, all the plots are related to the second one in Figure A.3. The first plot shows a "messy" plot where all the lines are connected and you can not eliminate the lines with convergence failure. The second plot was generated by my own

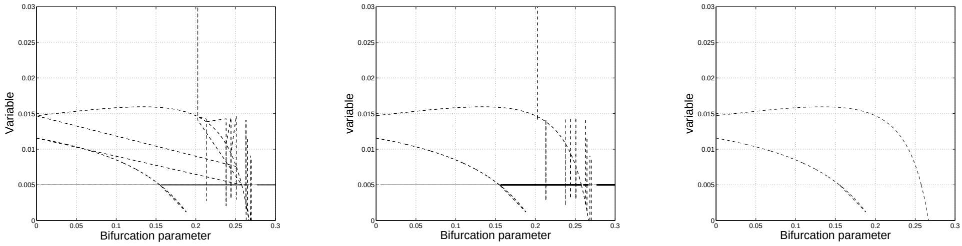

Figure A.4: “Make-up of plots”

code in matlab and as you can see all the lines are disconnected, allowing to cut the undesirable lines as showed in the third plot.

```
%Copyright by Flora Souza Bacelar
%Plot bifurcation diagrams in Matlab that have been saved by XPPAUT
%Tested Under Matlab version 7.4.0.287 (R2007a)

[file_in,path] = uigetfile('*.dat','.dat file saved by AUTO (XPPAUT)');
file_name = [path file_in];
 b=load(file_name);
linhas=size(b(:,1),1);
a=zeros(linhas+2,5);
a(1:linhas,1:5)=b(1:linhas,1:5);
figure;
 m=0;
for i=1:linhas+1

 if a(i,4)==a(i+1,4);
        m=m+1;
        c(m,1)=a(i,1);
        c(m,2)=a(i,2);
        c(m,3)=a(i,3);
        c(m,4)=a(i,5);
        else
```

```
m=m+1;
c(m,1)=a(i,1);
c(m,2)=a(i,2);
c(m,3)=a(i,3);
c(m,4)=a(i,5);
size(c(:,1),1);

 if a(i,4)==1 %STABLE STEADY STATE
      plot(c(:,1),c(:,[2 3]),'linestyle','-','linewidth',3,'color','k');
      hold on;
      elseif a(i,4)==2;%UNSTABLE STEADY STATE
      d=zeros(m+2,4);
      d(1:m,1:4)=c(1:m,1:4);
      n=0;
      for j=1:m+1
      if d(j,4)==d(j+1,4);
      n=n+1;
      f(n,1)=d(j,1);
      f(n,2)=d(j,2);
      f(n,3)=d(j,3);
      else
      n=n+1;
      f(n,1)=d(j,1);
      f(n,2)=d(j,2);
      f(n,3)=d(j,3);
      plot(f(:,1),f(:,[2 3]),'linestyle','--','linewidth',1,'color','k');
      hold on;
      f=zeros(1);
      n=0;
      end

end
elseif a(i,4)==3;%STABLE PERIODIC ORBIT
plot(c(1:5:length(c),1),c(1:5:length(c),[2 3]),'linestyle','o','linewidth',2,
'Markersize',8,'color','r','Markerfacecolor','r');
hold on;
else %a(i,4)==4;%UNSTABLE PERIODIC ORBIT
```

```
    plot(c(:,1),c(:,[2 3]),'linestyle','o','linewidth',2,'Markersize',8,'color','b');
    hold on;
    end
    c=zeros(1);
    m=0;
    grid on;
    axis tight
    end

end
```

Of course before starting bifurcation analysis with AUTO you might know your system making some analytical studies, when possible, and numerical analyzes in order to obtain the interesting parameter region in which the bifurcations are laid.

A.2 Matcont

Matcont is a freely available graphical Matlab package for the study of dynamical systems. This package can be downloaded from the webpage: http://www.matcont.ugent.be/.

Like XPPAUT, using this tool is possible to integrate numerically the equations and to do the continuation of equilibrium and periodic solutions with respect to a control parameter. Among many possibilities of this tool usage it is also possible continue a equilibrium in two and three control parameters.

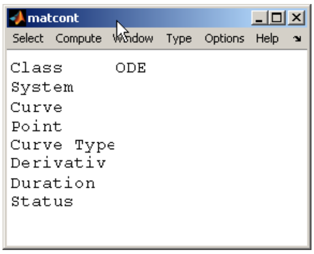

```
Class      ODE
System
Curve
Point
Curve Type
Derivativ
Duration
Status
```

Figure A.5: Matcont window.

Matcont contents a folder with some systems as an example. In order to write your own system, the better way to do it is choosing one among of the examples and then modify and rename it. In this way the steps you should follow are: open the Matcont window, see Figure A.5, choose

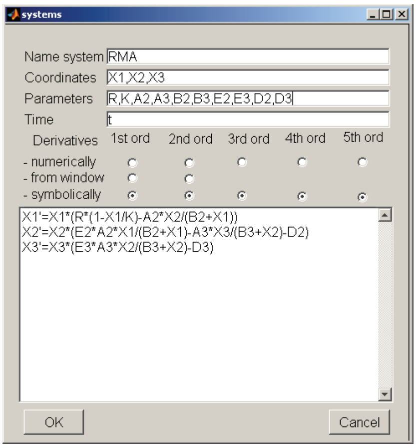

Name system: RMA
Coordinates: X1,X2,X3
Parameters: R,K,A2,A3,B2,B3,E2,E3,D2,D3
Time: t

Derivatives	1st ord	2nd ord	3rd ord	4th ord	5th ord
- numerically	○	○	○	○	○
- from window	○	○			
- symbolically	●	●	●	●	●

```
X1'=X1*(R*(1-X1/K)-A2*X2/(B2+X1))
X2'=X2*(E2*A2*X1/(B2+X1)-A3*X3/(B3+X2)-D2)
X3'=X3*(E3*A3*X2/(B3+X2)-D3)
```

Figure A.6: Matcont system window.

"Select" and then "Systems" and click in the option "Edit/Load" instead of the option "New". As a result a window, Figure A.6, will appear in which you can write your system.

Since you are in the Matlab platform, you can use all the graph tools therein. You can also see simultaneously the continuation evolution in all variables and in a three dimensional space, you just have to select the "window" option and add how many plots you want. With Matcont, you will not have problems with mixed data or lines in the plots. However, is better stop the process of continuation each bifurcation point. This allows you to access separately each branch of equilibria. So, after selecting the control parameter and the fixed point to continue, click "compute", then "forward". The calculation will stop when a bifurcation point is detected and a small window with three options will appear, see Figure A.7. Select "stop" option, and immediately, rename the present curve. To extend the curve select it and restart from the last point of the curve. This will permit you to access each branch of the curve in order to edit them separately.

Figure A.7. Matcont resume window.

In order to illustrate, see Figure A.8, that shows all the windows that compounds the Matcont tool.

There are other softwares that can be used to study dynamical systems, see the webpage http://www.dynamicalsystems.org/sw/sw/. All of them have advantages and disadvantages, you just might choose the one that fits your style of working. In the present thesis both XPPAUT and Matcont were used. Auto runs faster the continuations while Matcont seems to be more stable in the complicated range of parameters mentioned before.

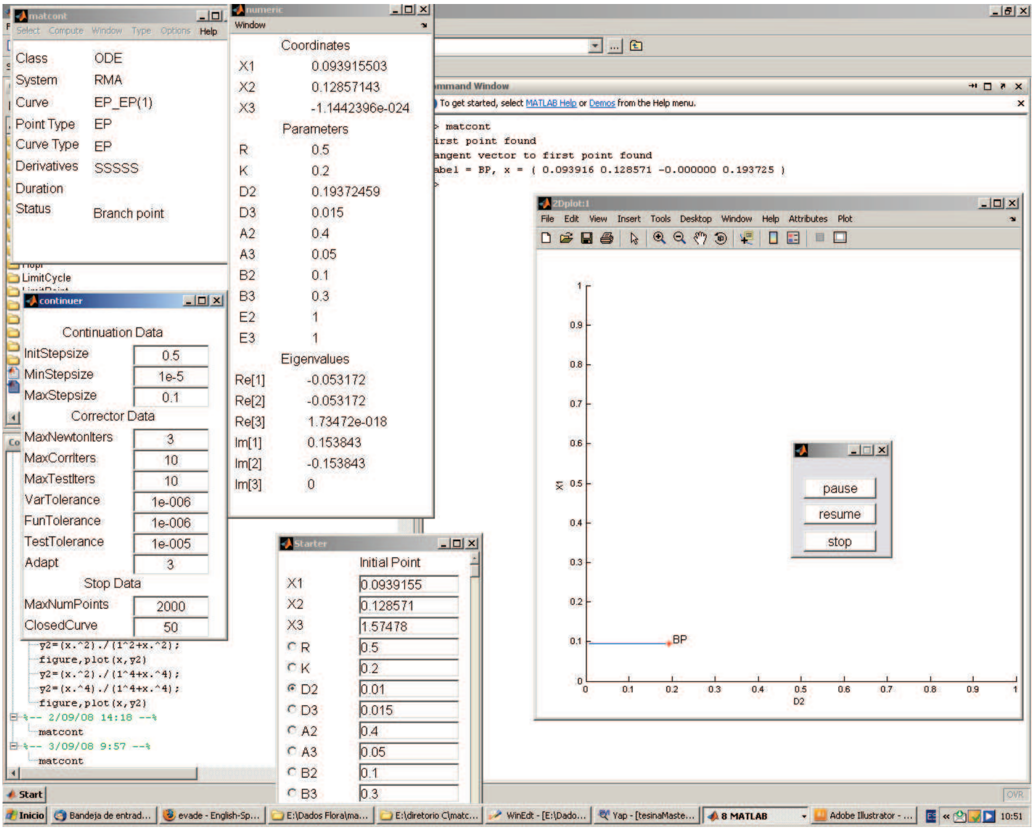

Class	ODE
System	RMA
Curve	EP_EP(1)
Point Type	EP
Curve Type	EP
Derivatives	SSSSS
Duration	
Status	Branch point

Coordinates	
X1	0.093915503
X2	0.12857143
X3	-1.1442396e-024
Parameters	
R	0.5
K	0.2
D2	0.19372459
D3	0.015
A2	0.4
A3	0.05
B2	0.1
B3	0.3
E2	1
E3	1
Eigenvalues	
Re[1]	-0.053172
Re[2]	-0.053172
Re[3]	1.73472e-018
Im[1]	0.153843
Im[2]	-0.153843
Im[3]	0

Continuation Data	
InitStepsize	0.5
MinStepsize	1e-5
MaxStepsize	0.1
Corrector Data	
MaxNewtonIters	3
MaxCorrIters	10
MaxTestIters	10
VarTolerance	1e-006
FunTolerance	1e-006
TestTolerance	1e-005
Adapt	3
Stop Data	
MaxNumPoints	2000
ClosedCurve	50

Initial Point	
X1	0.0939155
X2	0.128571
X3	1.57478
○ R	0.5
○ K	0.2
● D2	0.01
○ D3	0.015
○ A2	0.4
○ A3	0.05
○ B2	0.1
○ B3	0.3

```
To get started, select MATLAB Help or Demos from the Help menu.
> matcont
irst point found
angent vector to first point found
abel = BP, x = ( 0.093916 0.128571 -0.000000 0.193725 )
>
```

```
y2=(x.^2)./(1^2+x.^2);
figure,plot(x,y2)
y2=(x.^2)./(1^4+x.^4);
y2=(x.^4)./(1^4+x.^4);
figure,plot(x,y2)
%-- 2/09/08 14:18 --%
matcont
%-- 3/09/08 9:57 --%
matcont
```

Figure A.8: Matcont windows.

Bibliography

[1] A. Lyapunov, The General Problem of the Stability of Motion, Taylor and Francis, London, 1892.

[2] M. W. Hirsch, S. Smale, Differential equations, dynamical systems, and linear algebra, Academic Press, New York, 1974.

[3] S. H. Strogatz, Nonlinear dynamics and chaos: With applications to physics, biology, chemistry, and engineering, Perseus Books group, Cambridge, Massachusetts, 2000.

[4] A. A. Andronov, E. A. Leontovich, I. I. Gordon, A. G. Maier, Qualitative Theory of Second-Order Dynamic Systems, Wiley, New York, 1973.

[5] H. Poincaré, Sur l'équilibre d'une masse fluide animée d'un mouvement de rotation, Acta Mathematica 7 (1885) 259380.

[6] M. Peixoto, Structural stability on two-dimensional manifolds, Topology 1 (1962) 101–120.

[7] E. F. F. Hopf, Abzweigung einer periodischen losung van einer stationaren losung eines differential- systems, Berichte der Mathematisc- Physikalischen Konoglich-Sachsischen Academie der Wissenschaften Leipzig, 94 (1942) 1–22.

[8] H. Poincaré, Les méthodes nouvelles de la mécanique céleste, Gauthier-Villars, Paris, 1892.

[9] A. A. Andronov, Les cycles limites de poincar et la thorie des oscillations auto-entretenues, , , vol. , pp. ., Comptes Rendus de l'Acadmie des Sciences de Paris 189 (1929) 559–561.

[10] V. Melnikov, On the stability of the center for timeperiodic perturbations,

Tr. Moscow Math. Soc. 12 (1963) 3–52.

[11] J. K. Hale, H. Koçak, Dynamics and bifurcations, Springer-Verlag, New York, 1991.

[12] F. Takens, Singularities of vector fields, Pub. Math. IHES 43 (1974) 47–100.

[13] R. I. Bogdanov, Versal deformations of a singular point on the plane in the case of zero eigenvalues, Func. Anal. Appl. 9 (1975) 144–145.

[14] O. Rössler, An equation for continuous chaos, Physical Letters A 57 (1976) 397–398.

[15] D. P. Ruelle, F. Takens, On the nature of turbulence, Communications of Mathematical Physics 20 (1971) 167192.

[16] F. J. Romeiras, E. Ott, Strange nonchaotic attranctors of the damped pendulum with quasiperiodic forcing, Physical Review A 35 (10) (1987) 4404–4413.

[17] E. N. Lorenz, Determinisctic nonperiodic flow, Journal of the Atmosferic Sciences 20 (1963) 130–141.

[18] J. Thompson, H. Stewart, Nonlinear Dynamics and Chaos, 2nd Edition, John Wiley and Sons, Chichester, UK, 2002.

[19] J. Gugenheimer, P. Holmes, Nonlinear oscillations, dynamical systems and bifurcations of vector fields, Vol. 42, Applied mathematical sciences, Springer-Verlag, New York Inc, 1993.

[20] L. H. A. Monteiro, Systemas Dinâmicos, Editora Livraria da Física, São Paulo, 2006.

[21] A. Dhooge, W. Govaerts, Y. Kuznetsov, Matcont: A matlab package for numerical bifurcation analysis of odes., ACM Trans. Math. Software 29 (2003) 141 – 164.

[22] E. Doedel, A. Champneys, T. Fairgrieve, Y. Kuznetsov, B. Sandstede, X. Wang, Auto 97: continuation and bifurcation software for ordinary differential equations, Technical report, Concordia University, Montreal, Canada (1997).

[23] B. Ermentrout, Simulating, Analyzing, and Animating Dynamical Systems: A Guide to Xppaut for Researchers and Students (Software, Environments, Tools), SIAM: Society for Industrial and Applied Mathematical, 2002.

[24] T. R. Malthus, An Essay On The Principle Of Population as it Affects The Future Improvement of Society, J. Johnson, London, 1798.

[25] P. Turchin, Does population ecology have general laws?, Oikos 94 (2001) 17–26.

[26] B. Gompertz, On the nature of the function expressive of the law of human mortality, and on a new mode of determining the value of life contingencies, Philosophical Transactions of the Royal Society of London 115 (1825) 513–585.

[27] C. P. Winsor, The Gompertz curve as a growth curve, Proceedings of the national academy of sciences 18 (1) (1932) 1–8.

[28] G. C. Chow, Technological change and the demand for computers, The American Economic Review 57 (5) (1967) 1117–1130.

[29] P. W. Durbin, N. Jeung, M. H. Williams, J. S. Arnold, Construction of a growth curve for mammary tumors of the rat, Cancer Research 27 (1967) 1341–1347.

[30] P. F. Verhuslt, Notice sur la loi que la population suit dans son accroissement, Correpondance mathematique et Physique 10 (1838) 112–121.

[31] R. Pearl, L. J. Reed, On the rate of growth of the population of the united states since 1790 and its mathematical representation, Proceedings of the National Academy of Sciences 6 (6).

[32] P. E. Stranndberg, The chemostat, Tech. rep., Univeristy of Linköping, Sweden (2003).

[33] M. A. Savageau, Growth equations: A general equation and a survey of special cases, Mathematical Biosciences 48 (1980) 267–278.

[34] A. J. Lotka, Elements of physical biology, Williams and Wilkins, Baltimore, 1925.

[35] V. Volterra, Fluctuations in the abundance of a species considered mathematically, Nature 118 558–60.

[36] C. S. Holling, Resilience and stability of ecological systems, Annual Review of Ecologly and Systematics 4 (1973) 1–23.

[37] C. S. Holling, The functional response of predators to prey density and its role in mimicry and population regulation, Memoir of the Entomological Society of Canada 45 (1965) 1–60.

[38] C. S. Holling, The components of predation as revealed by a study of small-mammal predation of the european pine sawfly, The Canadian Entomologist 91 (7) (1959) 293–320.

[39] C. S. Holling, Some characteristics of simple types of predation and parasitism, The Canadian Entomologist 91 (7) (1959) 385–398.

[40] G. F. Gause, The Struggle for Existence, Willianms and wilkins, Baltimore,

1934.

[41] M. L. Rosenzweig, Paradox of enrichment: destabilization of exploitation ecosystems in ecological time, Science 171 (1971) 385–387.

[42] K. E. F. Watt, A mathematical model for the effect of densities of attacked and attacking species on the number attacked, Canadian Entomologist 91 (1959) 129–144.

[43] R. M. May, Limit cycles in predator-prey communities, Science 177.

[44] Y. Nishiuchi, T. Ueta, H. Kawakami, Stable torus and its bifurcation phenomena in a simple three-dimensional autonomous circuit, Chaos, Solitons and Fractals 27 (2006) 941951.

[45] J. S. Gunnarsson, D.Broman, P. Jonsson, M. Olsson, R. Rosenberg, Interactions between eutrophication and contaminants: towards a new research concept for the european aquatic environment.

[46] J. W. Fleeger, K. Carman, R.M.Nisbet, Indirect effects of contaminants in aquatic ecosystems, The Science of the Total Environment 317 (2003) 207–233.

[47] B. D. Fath, Network mutualism: Positive community-level relations in ecosystems, Ecological Modelling 208 (2007) 56–67.

[48] J. B. C. Jackson, M. X. Kirby, W. Berger, K. Bjorndal, L. W. Botsford, B. J. Bourque, R. H. Bradbury, R. Cooke, J. Erlandson, J. A. Estes, T. P. Hughes, S. Kidwell, C. B. Lange, H. S. Lenihan, J. M. Pandolfi, C. H. Peterson, R. S. Steneck, M. J. Tegner, R. R. Warner, Historical overfishing and the recent collapse of coastal ecosystems, Science 293 (2001) 629–638.

[49] G. M. Daskalov, Overfishing drives a trophic cascade in the Black sea, Marine Ecology Progress Series 225 (2002) 53–63.

[50] M. Scheffer, S. R. Carpenter, Catastrophic regime shifts in ecosystems: linking theory to observation, Trends in Ecology and Evolution 18 (2003) 648–656.

[51] M. Scheffer, S. R. Carpenter, J. A. Foley, C. Folke, B. Walker, Catastrophic shifts in ecosystems, Nature 413 (2001) 591–596.

[52] G. W. S. II, Ecological Risk Assessment, Lewis Publishers,Boca Raton, Florida, 1993.

[53] G. F. Fussmann, G. Heber, Food web complexity and chaotic population dynamics, Ecology Letters 5 (2002) 394–401.

[54] J. M. Zaldívar, E. Cattaneo, M. Plus, C. N. Murray, G. Giordani, P. Viaroli,

Long-term simulation of main biogeochemical events in a coastal lagoon: Sacca di goro(Northern Adriatic coast, Italy), Continental Shelf Research 23 (2003) 1847–1876.

[55] R. P. Canale, An analysis of models describing predator-prey interaction, Biotechnology and Bioengineering 12 (1970) 353–358.

[56] M. P. Boer, B. W. Kooi, S. A. L. M. Kooijman, Food chain dynamics in the chemostat, Mathematical Biosciences 150 (1998) 43–62.

[57] M. P. Boer, B. W. Kooi, S. A. L. M. Kooijman, Multiple attractor and boundary crises in a tri-trophic food chain, Mathematical Biosciences 169 (2001) 109–128.

[58] A. Hastings, T. Powell, Chaos in a three-species food chain, Ecology 72(3) (1991) 896–903.

[59] A. Klebanoff, A. Hastings, Chaos in three-species food chains, Journal of Mathematical Biology 32 (5) (1994) 427–451.

[60] P. A. Abrams, J. D. Roth, The effects of enrichment of three-species food chains with non-linear functional responses, Ecology 75 (1994) 1118–1130.

[61] K. McCann, P. Yodzis, Biological conditions for chaos in a three-species food chain, Ecology 75 (2) (1994) 561–564.

[62] Y. A. Kuznetsov, S. Rinaldi, Remarks on food chain dynamics, Mathematical Biosciences 134 (1996) 1–33.

[63] O. DeFeo, S. Rinaldi, Yield and dynamics of tritrophic food chains, The American Naturalist 150 (3) (1997) 328–345.

[64] A. Gragnani, O. D. Feo, S. Rinaldi, Food chain dynamics in the chemostat: Relationships between mean yield and complex dynamics, Bulletin of Mathematical Biology 60 (1998) 703–719.

[65] C. R. Gwaaltney, M. P. Styczynski, M. A. Stadtherr, Reliable computation of equilibrium states and bifurcations in food chain models, Computers ℘ Chemical Engineering 28 (2004) 1981–1996.

[66] E. Mosekilde, Topics in Nonlinear Dynamics. Application to Physics, Biology and Economic Systems, World Scientific publishing, Singapore, 1998.

[67] I. D. Lima, D. B. Olson, S. C. Doney, Intrinsic dynamics and stability properties of size-structured pelagic ecosystem models, Journal of Plankton Research 24 (6) (2002) 533–556.

[68] Y. A. Kuznetsov, O. D. Feo, S. Rinaldi, Belyakov homoclinic bifurcations in a tritrophic food chain model, SIAM Journal on Applied Mathematics 62

(2001) 462–487.

[69] C. X. J. Jensen, L. R. Ginzburg, Paradoxes or theoretical failure? the jury is still out, Ecological Modelling 188 (2005) 3–14.

[70] G. F. Fussmann, S. P. Ellner, K. W. Sherzer, N. G. H. Jr, Crossing the Hopf bifurcation in a live predator-prey system, Science 290 (2000) 1358–1360.

[71] K. W. Shertzer, S. P. Ellner, G. F. Fussmann, N. G. H. Jr, Predator-prey cycles in an aquatic microcosm: testing hypotheses of mechanism, Journal of Animal Ecology 71 (2002) 802–815.

[72] T. Bell, The ecological consequences of unpalatable prey: phytoplankton response to nutrient and predator additions, Oikos 99 (2002) 59–68.

[73] K. L. Kirk, Enrichment can stabilize population dynamics: autotoxins and density dependence, Ecology 79 (7) (1998) 2456–2462.

[74] R. K. Upadhayay, J. Chattopadhayay, Chaos to order: role of toxin producing phytoplankton in aquatic systems, Nonlinear analysis: modeling and control 10 (4) (2005) 383–396.

Index

Curriculum vitae

Flora Souza Bacelar

Personal Information

Date of birth:	04/01/1978
Place of birth:	Salvador of Bahia
Country:	Brazil
E-mail:	florabacelar@ifisc.uib-csic.es
URL:	http://www.ifisc.uib-csic.es/people/people-detail.php?id=585

Education

- (January 2001) Graduate in Physics.
  Universidade Federal da Bahia (UFBA-Brazil).
- (October 2004) Master degree in Physics.
  Universidade Federal da Bahia (UFBA-Brazil).
  Thesis Advisor: Prof. Rorberto Fernandes Silva Andrade.

- (Since January 2006) PHD Student in Physics.
  Universitat de les Illes Balears, Palma de Mallorca.
  Thesis Advisor: Prof. Emilio Hernández García.

Current Affiliation

- ORGANISM:Universitat de les Illes Balears (UIB)
- CENTER: : Instituto de Fsica Interdisciplinar y Sistemas Complejos, *IFISC*, (CSIC-UIB)
- PROFESSIONAL CATEGORY AND STARTING DATE: PhD student at the UIB and scholarship holder of a Fellowship from the Government of the Balearic Islands since 01/09/2007. PhD supervisor: Prof. Emilio Hernández García .
- POSTAL ADDRESS:

  Instituto de Física Interdisciplinar y Sistemas Complejos (IFISC)
  Ed. Mateu Orfila
  Campus UIB. Carretera de Valldemosa km. 7.5.
  07122-Palma de Mallorca
- PHONE: +34 971 173 369
- FAX: +34 971 173 426

Awarded Fellowships

1. "Iniciação científica" . Scholarship sponsor: PIBIC
   (Programa Institucional de Bolsas de Iniciação Científica),
   http://www.prp.unicamp.br/pibic/.
   PERIOD: 09/1998-08/1999.
   CENTER: Universidade Federal da Bahia (UFBA-Brazil).
   TITLE:"Caracterização de Fotomultiplicadoras".
   SUPERVISOR: Iuri Muniz Pepe.

2. “Iniciação científica” . Scholarship sponsor: PIBIC
   (Programa Institucional de Bolsas de Iniciação Científica),
   http://www.prp.unicamp.br/pibic/.
   PERIOD: 09/1999-08/2000.
   CENTER: Universidade Federal da Bahia (UFBA-Brazil).
   TITLE: “Desenvolvimento de instrumentação para detecção de luz de baixa intensidade”.
   SUPERVISOR: Iuri Muniz Pepe.

3. “Iniciação científica” . Scholarship sponsor: PIBIC
   (Programa Institucional de Bolsas de Iniciação Científica),
   http://www.prp.unicamp.br/pibic/.
   PERIOD: 09/2000-08/2001.
   CENTER: Universidade Federal da Bahia (UFBA-Brazil).
   TITLE:“Propriedades óticas e de transporte de sistemas semicondutores”.
   SUPERVISOR: Antonio Ferrera da Silva.

4. Master of Physics. Scholarship sponsor: CNPQ
   (Conselho Nacional de Desenvolvimento Científico e Tecnológico),
   http://www.cnpq.br/.
   PERIOD: 09/2001-12/2003.
   CENTER: Universidade Federal da Bahia (UFBA-Brazil).
   TITLE: “Um modelo de equações diferenciais funcionais com retardo temporal para a dinâmica de infecção pelo VIH ”.
   SUPERVISOR: Rorberto Fernandes Silva Andrade.

5. PHD studies. Scholarship sponsor: European community.
   THRESHOLDS integrated project(Thresholds of Environmental Sustainability), http://www.thresholds-eu.org/index.html.
   PERIOD: 01/02/2006-30/09/2007.
   CENTER: Instituto Mediterraneo de Estudios Avanzados (CSIC-IMEDEA)-Cross-Disciplinary Physics Department.
   SUPERVISOR: Emilio Hernández García .

Research Lines

- Nonlinear Dynamics
- Statistical Physics
- Biological Modeling
- Bifurcation theory of dynamical systems
- Stochastic Differential Equations
- Delay differential equations
- Spatial differential equations
- Individual-based models (CA)

Participation in Research Projects

1. ”Física Biologica”. Program: 28001010002P-5 FSICA - UFBA (2004) Coordinator: Suani Tavares Rubim de Pinho.
2. THRESHOLDS: Thresholds of environmental sustainability Integrated Project (Contract 003933), VI Framework Program, European Union. Priority 6.3 Global Change and Ecosystems” (2005-2008). Coordinator: C. Duarte (RRNN-IMEDEA). Responsible workpackage S2WP1 ’Regime modelling’: E.Hernández-García.
3. Grupo de investigación competitivo de Física Interdisciplinar (Grupo de Excelencia Coherente). Subvención del Govern Balear (2006-2008). Investigador principal : M. San Miguel.
4. Fisicos: Física Interdisciplinar de Sistemas Complejos. Proyecto Fis2007-60327, Ministério de Educación y Ciencia. Investigador principal: M. San Miguel.

Teaching Experience

1. Classical Mechanics 1. Federal University of Bahia (UFBA), (Brazil). 05/01/2004-05/01/2006.
2. Classical Mechanics 1. Centro Baiano de Ensino Superior (AREA1), (Brazil). 01/03/2005-02/01/2006.
3. Electromagnetism. Centro Baiano de Ensino Superior (AREA1), (Brazil). 01/07/2005-02/01/2006.

Stays at foreign research centers

- From 10/05/2006 to 12/05/2006 under the supervision of Professor José-Manuel Zaldívar, Institute for Environment and Sustainability, Joint Research Center of the European Commission, Ispra (Italy).
- From 17/11/2006 to 22/11/2006 under the supervision of Professor José-Manuel Zaldívar, Institute for Environment and Sustainability, Joint Research Center of the European Commission, Ispra (Italy).
- From 25/07/2007 to 27/07/2007 under the supervision of Professor José-Manuel Zaldívar, Institute for Environment and Sustainability, Joint Research Center of the European Commission, Ispra (Italy).

`Schools`

- Summer School -PHYSBIO - Stochastic processes, fluctuations and noise, St. Etienne, France, 13. Aug. - 08. Oct. 2006
- Transylvanian Summer School Series - International Workshop on Complex Systems and Networks, Sovata, Romania, July 15-20, 2007.

Submited Papers

1. Zaldívar, J.M.;Bacelar, F.S.; Dueri, S.; Marinov, D.; Viaroli, P.; Hernández-García, E.. "*A modeling approach to nutrient and temperature driven regime shifts in shallow coastal ecosystems: Competition between seagrass and macroalgae*", (2008).

2. Bacelar, F.S.; Dueri, S.;Hernndez-Garca, E. ; Zaldvar,J.M.. " *Joint effects of nutrients and contaminants on the dynamics of a food chain in marine ecosystems*",(2008).

Conference Presentations

[O] = Oral presentation, [P] = Poster presentation

1. "*Caracterização de Fotomultiplicadoras*", XVIII Seminário estudantil, UFBA, Brazil. October (1999). [O]

2. "*Desenvolvimento de instrumentação para detecção de luz de baixa intensidade*", XIX Seminário estudiantil, UFBA, Brazil. October de (2000). [O]

3. "*Propriedades óticas e de transporte de sistemas semicondutores*", XIX Seminário estudantil, UFBA, (Brazil), March (2002). [P]

4. "*Estudo de um modelo de equações diferenciais ordinárias para descrever a dinâmica de infecção pelo HIV*", XXVI encontro Nacional de Física da matéria condensada, Poços de Caldas, (Brazil), May (2004). [P]

5. "*Estudo de um modelo de equações diferenciais ordinárias para descrever a dinâmica de infecção pelo VIH*", II Bienal da Sociedade Brasileira de Matemática, UFBA, (Brazil), 27 octuber (2004). [P]

6. "*Duas escalas de tempo em um modelo de equações diferenciais com retardo temporal para a infecção pelo VIH*", XXII Encontro de Físicos do Norte e Nordeste, Feira de Santana-Ba, (Brazil), 08-12 november (2004). [P]

7. "*Duas Escalas de tempo em um modelo de equações diferenciais com retardo temporal para infecção pelo VIH*", X Congresso Brasileiro de Física Médica poster, Salvador, (Brazil). 26-29 may (2005). [P]

8. "*Analise comparativa de modelos angiogênicos de diferentes terapias do câncer*", XXIII Encontro de Físicos do Norte e Nordeste", Maceió-Al, Brazil. October (2005). [O]

9. Presented by S. T. R. PINHO "*A comparative analysis of nonlinear time delayed angiogenic models of cancer therapies*", PINHO, S. T. R. ; BACELAR, Flora Souza ; ANDRADE, R. F. S..
   XIX Latin American Workshop on Nonlinear Phenomena (LAWNP05), Bariloche (Argentina), (2005). [O]

10. Presented by R. F. S. Andrade "*Investigations on the HIV dynamics with a system of time delayed differential equations* ", Andrade, R. F. S.; BACELAR, Flora Souza ; SANTOS, Rita Maria Zorzenon
    Work shop on Immunology, International centre of condensed matter physics, Brasilia (Brazil), (2005). [O]

11. Presented by S. T. R. PINHO "*Ação Angiogênica em Modelos de Terapias de Câncer*", PINHO, S. T. R. ; ANDRADE, Roberto Fernandes Silva ; BACELAR, Flora Souza .
    XXIX Encontro Nacioanl de Física da Matéria Condensada (XXIX ENFMC), São Lourenço (Brazil), (2006). [O]

12. "*Integration of Langevin Equations with Multiplicative noise: Using a split-step scheme*", PHYSBIO- Non-equilibrium in Physics and in Biology, St. Etienne, France. October (2006). [O]

13. "*A comparative Analysis of time-delayed models of cancer therapies at the vascular stage. 2nd Conference of the BioSim Network of Excellence*", Calas Viñas, Mallorca (Spain). 18-22 October (2006). [P]

14. Presented by J.-M. Zaldivar-Comenges "*A modelling approach to nutrient-driven regime shifts in shallow coastal systems: competition between seagrass and macroalgae*", J.-M. Zaldívar-Comenges, F.S. Bacelar, S. Dueri, E. Hernández-García, P. Viaroli.

6th International Congress on Industrial and Applied Mathematics (ICIAM07). Zurich, (Switzerland). 16-20 July (2007). [P]

15. Presented by E. Hernández-García "*Regime changes in competing floating-submerged plant ecosystems*", F.S. Bacelar, J.-M. Zaldívar-Comenges, S. Dueri, E. Hernández-García.
European Conference on Complex Systems (ECCS07). Dresden, Germany, 30 September - 6 October (2007). [P]

16. "*Regime changes in competing floating-submerged plant ecosystems*", F. S.Bacelar, J.-M. Zaldívar-Comenges, S. Dueri, E. Hernández-García. FisEs'08 Salamanca, 27 -29 de Marzo de (2008). [P]

17. "*Join effects of nutrients and contaminants on the dynamics of a food chain in marine ecosystems* ", Flora S. Bacelar, Sibylle Dueri, Emilio Hernández-García and José-Manuel Zaldívar. FisEs'08 Salamanca, 27 -29 de Marzo de (2008). [P]

Computer Skills

- Programming languages: Fortran 77, Python,
- Operating systems: Windows.
- Mathematics: Matlab, Mathematica.
- Typesetting: LaTeX, Word.

Last updated: September 9, 2008

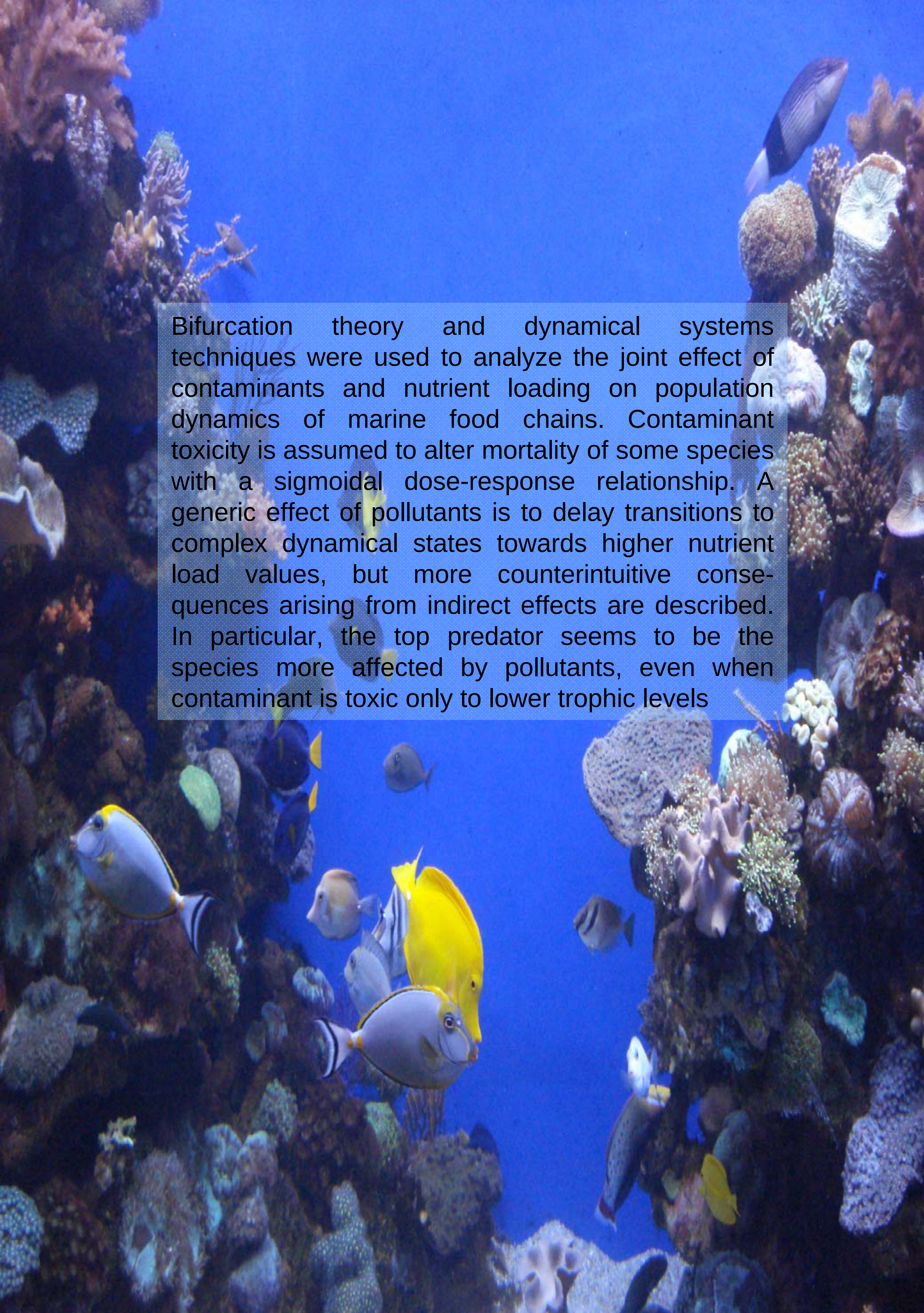

Bifurcation theory and dynamical systems techniques were used to analyze the joint effect of contaminants and nutrient loading on population dynamics of marine food chains. Contaminant toxicity is assumed to alter mortality of some species with a sigmoidal dose-response relationship. A generic effect of pollutants is to delay transitions to complex dynamical states towards higher nutrient load values, but more counterintuitive consequences arising from indirect effects are described. In particular, the top predator seems to be the species more affected by pollutants, even when contaminant is toxic only to lower trophic levels